Synthetic lethal screening identifies existing autophagy drugs with selective viability effects on Neurofibromatosis type-1 model systems

Wang, Y.[1,2,†], Stevens, M.[1,3,†], Mandigo, T.R.[4], Bouley, S.J.[4], Sharma, A.[4], Sengupta, S.[1,3], Housden, A.[1], Perrimon, N.[5,6], Walker, J.A.[4,7]*, Housden, B.E.[1,3,]*

[1] The Living Systems Institute, University of Exeter, Exeter, UK
[2] The First People's Hospital of Qinzhou, China
[3] The College of Medicine and Health, University of Exeter, Exeter, UK
[4] Center for Genomic Medicine, Massachusetts General Hospital, Boston, MA 02114, USA
[5] Department of Genetics, Blavatnik Institute, Harvard Medical School, Boston, MA, 02115, USA
[6] Howard Hughes Medical Institute
[7] Cancer Program, Broad Institute of MIT and Harvard, Cambridge, MA 02142, USA

[†] These authors contributed equally
* Correspondence to b.housden@exeter.ac.uk and jwalker@helix.mgh.harvard.edu

Key Words
Neurofibromatosis type 1; Synthetic lethality; Drug repurposing; Drosophila; Autophagy

ABSTRACT

Neurofibromatosis type 1 (NF1) is a genetic disorder associated with a variety of symptoms including the formation of benign tumours. Drug treatments are currently limited and there is a clear need to discover new drugs to target NF1-deficient tumour cells. Using a *Drosophila* cell model of NF1, we performed synthetic lethal screens to identify novel drug targets. We identified 54 candidates, five of could be targeted with existing drugs, including autophagy inhibitors. Inhibition of autophagy using Chloroquine (CQ) resulted in selective reduction in cell viability in a panel of human NF1 mutant cell lines and a *Drosophila in vivo* model. Finally, we found that combined treatment with CQ and selumetinib resulted in further reduction of NF1 mutant cell viability. The results of this study highlight two key points: 1) the use of *Drosophila* cells as a model to screen for drugs specifically targeting *NF1* mutant cells was highly successful as the candidate interactions were conserved across a panel of human *NF1* mutant cells and an *in vivo* fly *NF1* mutant model, and 2) NF1-deficient cells have vulnerability to disruption of the autophagy pathway. Not only does this pathway represent a promising target for the treatment of NF1-associated tumours, but we identified CQ and bafilomycin A1 as candidate drugs for the treatment of NF1 tumours.

INTRODUCTION

Neurofibromatosis type 1 (NF1) [1], is a genetic disorder with autosomal-dominant inheritance affecting 1 in ~3,000 [2]. Although the penetrance of NF1 is virtually complete after childhood, the disease is characterized by highly variable clinical expressivity. Symptoms include near universal benign, but often disfiguring, peripheral nerve associated tumours known as neurofibromas, as well as malignant tumours, including usually fatal malignant peripheral nerve sheath tumours (MPNSTs). While the tumour suppressor role of NF1 has received much attention, NF1 is a multi-system disorder where non-tumour symptoms contribute significantly to its morbidity. These non-tumour symptoms include skeletal and vascular abnormalities, pigmentation defects, reduced overall growth, and cognitive deficits, with the latter seen in 50-70% of children with NF1 [3]. In part reflecting higher rates of vascular defects and cancer, the life expectancy of NF1 patients is reduced by 15-20 years [4].

NF1 is caused by loss of neurofibromin, a 320 kDa protein whose only widely accepted function is to serve as a Ras GTPase Activating Protein (RasGAP) for H-, K-, N-Ras and R-Ras1, 2 and 3 [5]. RasGAPs promote the conversion of active Ras-GTP into inactive Ras-GDP by stimulating the low intrinsic rate of Ras-GTP hydrolysis [6]. Consequently, loss of neurofibromin can result in misregulation of signalling downstream of Ras, the best documented being the RAF/MEK/ERK and PI3K/AKT/mTOR pathways. Although dysregulated Ras signalling is believed to be the proximal cause of NF1 symptoms, it is unclear which of the numerous effectors downstream of Ras are relevant for disease progression, as well as the identities of the disease-pertinent targets of the signalling pathways mediating their effects. The situation is further complicated since there is undoubtedly crosstalk between these different pathways. In patients with *NF1*-driven malignant tumours, targeting Ras pathway components such as MEK or ERK is a reasonable therapeutic option, although Ras is subject to highly robust regulation [6], which may explain why, despite considerable effort, no effective therapy for Ras-driven cancers has yet emerged. However, chronically blocking Ras may never be an appropriate strategy for treating the many serious but non-life-threatening symptoms of NF1, especially in children.

Currently, there are limited therapies for any NF1-associated tumours. The only available drug is the MEK inhibitor selumetinib, which was approved for use in a subset of paediatric plexiform neurofibromas in April 2020. However, not all tumours were responsive to treatment and serious side effects can be associated with selumetinib use [7, 8]. Therefore, there is a clear clinical need to discover new drugs that specifically target NF1-deficient tumour cells either alone or in combination.

One approach to identify candidate drug targets for tumorigenic diseases is to use synthetic lethal interaction screens. Synthetic lethal interactions are a type of genetic interaction in which inhibition of either of two genes alone is viable, but the combined inhibition of both genes is inviable. When one of these genes is mutated in tumour cells, such interactions can be exploited to kill those cells exclusively by targeting the synthetic lethal partner gene using a drug [9]. This approach is attractive because treatment is expected to be lethal to tumour cells but have no effect on wild-type, healthy cells.

Despite long-term interest in the use of synthetic lethality as a therapeutic strategy to treat tumours, few drugs have successfully progressed to clinical use. One example are PARP inhibitors, which exploit a synthetic lethal interaction between the DNA damage repair pathway and *BRCA1/2*, which are often mutated in breast and ovarian cancers [10]. However, a major factor preventing successful development of treatments against synthetic lethal interactions is a lack of consistency between interactions identified in different genetic backgrounds [11]. This results in a lack of translation of candidate targets between model systems. Our approach to overcome this limitation makes use of *Drosophila* cells to initially identify synthetic lethal interactions with genes mutated in tumours. The reduced redundancy between gene functions in *Drosophila* permits the identification of interactions using RNA interference (RNAi) that may be otherwise hidden in human cells. The conservation of candidate interactions can then be assessed in a range of other model systems including human cells, providing a filter to remove interactions that are specific to a single model system. This approach has previously proved successful, leading to the discovery of mizoribine and palbociclib as promising candidates for the treatment of tuberous sclerosis complex (TSC) and VHL-linked cancers respectively [12, 13, 14]. In both cases, hits from *Drosophila* synthetic lethal screens were validated with a high success rate in both human cells and mouse models.

Given the previous success of using the *Drosophila* approach, we have applied this method to identify candidate drug targets to treat NF1-deficient tumours. Here, we describe the generation of a NF1 null mutant *Drosophila* cell line using CRISPR and its use in synthetic lethal screens to identify candidate drug targets to specifically kill NF1-associated tumour cells. We find that inhibition of autophagy (using chloroquine (CQ) and bafilomycin A1) has a selective effect on both a NF1-deficient *Drosophila* cell line and in an *in vivo* fly model. Furthermore, we show that this selective effect is conserved in multiple human tumour-derived cell lines, indicating that these repurposed drugs may have promise for the treatment of NF1 tumours in the future.

RESULTS

Generation of a *Drosophila* NF1 cell model cell using CRISPR/Cas9 gene editing

Our previous studies have demonstrated the potential of using cross-species genetic screens to identify candidate therapeutic targets for human disease [13, 14, 15]. The *NF1* gene is well conserved between *Drosophila* and humans with 68% identity at the amino acid level (**Fig. S1**). To use the same approach to find new targets for the treatment of NF1-associated tumours, we first used CRISPR gene editing to generate mutations in *dNF1* in a *Drosophila* cell line. S2R+ cells were transfected with Cas9 and a sgRNA designed to generate a double-strand break in exon 2 of *dNF1* (**Fig. 1A**). Briefly, transfected cells expressing high levels of CRISPR reagents were isolated using FACS and single-cell cloned, as described previously [14, 16]. Clones were assessed using high-resolution melting analysis (HRMA) to identify those carrying mutations at the target locus. Finally, sequencing was used to confirm that induced mutations were homozygous and resulted in frameshifts in *NF1* (**Fig. 1A**). Of note, S2R+ cells are aneuploid [17] and we found that they have three copies of the *dNF1* gene.

The resulting NF1-KO S2R+ cell line (hereafter called dNF1-KO) was characterized by assessing the expression of neurofibromin using western blots. We found no detectable signal in the dNF1-KO line when compared to parental WT S2R+ cells (**Fig. 1B**). Given that neurofibromin is a negative regulator of Ras, we assessed the growth and proliferative phenotypes of dNF1-KO cells compared to S2R+ cells. Consistent with deregulation of a mitogenic pathway, dNF1-KO cells showed an increased rate of growth as measured using CellTiter-Glo assays to assess total ATP levels in the population. This effect was observed in the absence of serum in the culture media and in the presence of serum (**Fig. 1C**), indicating that culture growth is both accelerated in the absence of NF1 and is decoupled from upstream growth factor signalling pathways. To determine whether this increase in culture growth was due to increased proliferation, increased cell growth or both, we performed cell counts following culture in full serum and CellTiter-Glo assays on normalised numbers of cells from each genotype (baseline readings). Cell counts for dNF1-KO showed an increase in cell numbers following culture compared to S2R+ cells and the ‘baseline’ CellTiter-Glo showed no difference (**Fig. 1C**). This suggests that the difference in culture growth is primarily due to increased cell proliferation rather than an increase in cell size or ATP content of the cells. Together, these results indicate that the dNF1-KO line represents a novel NF1 null mutant cell model, with properties consistent with known effects of NF1 loss.

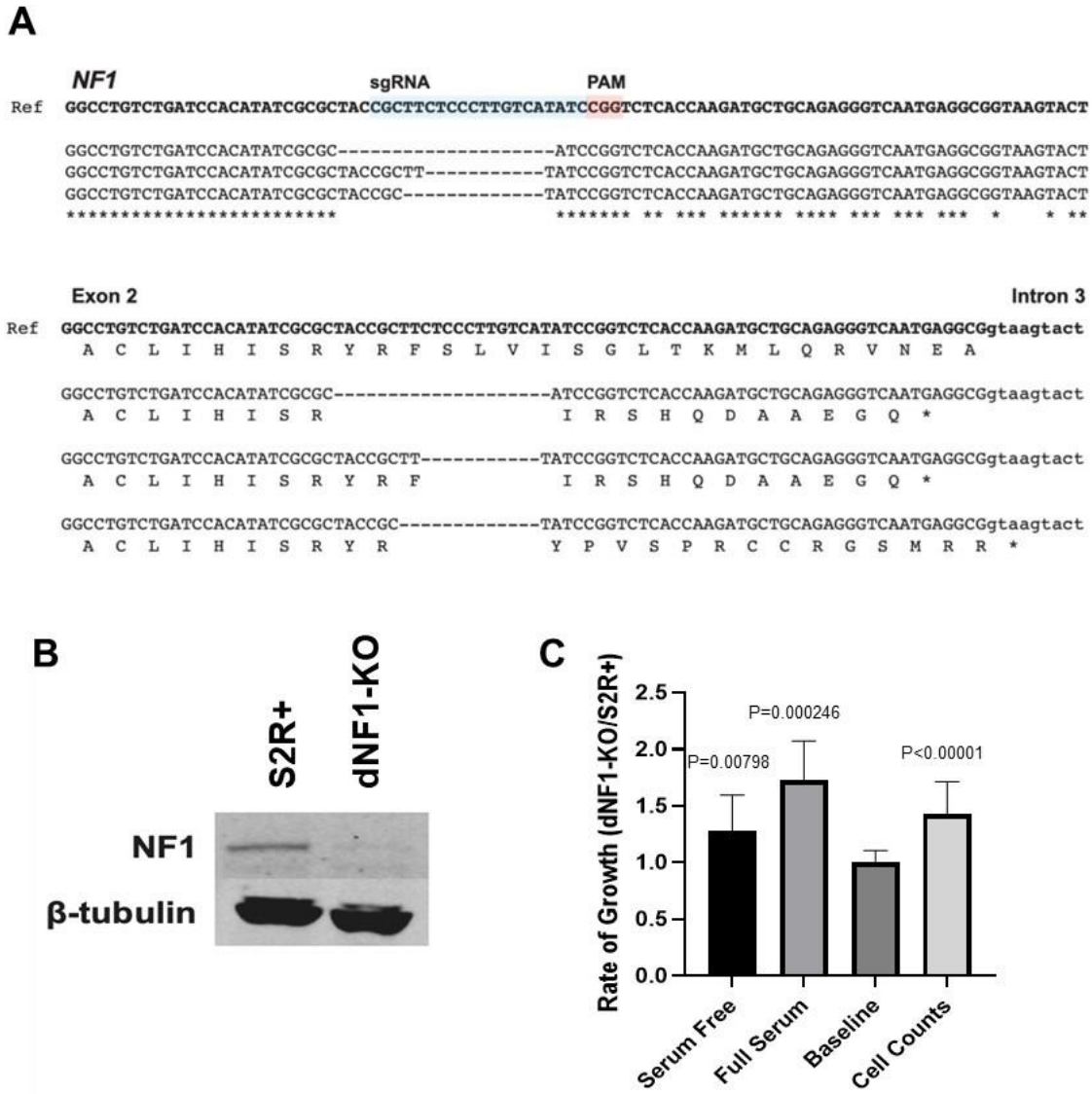

Figure 1. Characterisation of NF1-deficient *Drosophila* cells.

(A) S2R+ cells were transfected with Cas9 and sgRNA designed to target a double-strand break to a region close to the 5' end of the *NF1* coding sequence. **(B)** Representative image of Western blot showing loss of neurofibromin in dNF1-KO cells compared to WT S2R+ cells (two replicates performed). **(C)** Characterisation of dNF1-KO cell size and proliferation rate. Bars indicate the average of at least eight biological replicates and error bars indicate SD. (P values determined using paired, two-tailed t-tests. Baseline: n=60, Serum-free: n=50, Full-serum: n=42, Cell Counts: n=8).

Mapping synthetic lethal interactions in dNF1-KO cells using a genome-wide RNAi screen

We used our dNF1-KO cell line to screen for synthetic lethal interactions. We used a genome-wide dsRNA library to screen in both S2R+ and dNF1-KO cells (**Fig. 2A**). Screens were

performed in triplicate to allow identification of reproducible results. First, we normalised results to the median of each row and column to remove position effects and scale results from all assay plates to allow direct comparison (see methods for details). Z-scores were then calculated for each dsRNA reagent for each replicate screen and correlation between replicates was used to assess the quality of screen results. We note that some assay plates were affected by position effects. These were identified manually and removed from the analysis prior to correlation analysis. Correlation coefficients ranged between 0.9 and 0.99 (average 0.93) for control wells and between 0.55 and 0.66 (average 0.61) for non-control wells (**Fig. 2B-C**), illustrating a high rate of reproducibility between replicates. Next, we identified synthetic lethal interactions by filtering the results for dsRNA reagents that reduce the viability of dNF1-KO cells (median $Z<-1.5$) to a greater extent than wild-type cells (median $Z\geq-1.5$). This analysis identified 134 candidate genes (**Table S1**).

Genetic screens are often associated with false-positive results due to off-target effects from dsRNA reagents or noise in the screen assay. To remove potential false positives, we overlaid the screen hits onto a protein-protein interaction network from the String database [18]. Synthetic lethal interactions are generally similar between genes that have related functions. Therefore, proteins that physically interact are expected to share synthetic lethal interactions. Using the combination of physical and genetic interaction data, we can therefore remove false positives from the screen results by isolating only hits that have physical interactions with at least one other hit from the genetic interaction screen. In addition, we filtered the candidates to isolate only those with clear orthologs in humans. Following this process, 54 high-confidence candidate targets remained (**Fig. 2D, Table S2**).

Validation of candidate synthetic lethal interactions using Variable Dose Analysis (VDA)

To assess the validity of the network, we tested seven highly ranked genes based on the difference in median Z-score between dNF1-KO and S2R+ cells with various biological functions using variable dose analysis (VDA) assays [19] (**Table 1**). shRNA-expressing plasmids were generated targeting each of the seven genes and were transfected into S2R+ and dNF1-KO cells in combination with shRNA against *NF1* or against a negative control gene (*white*). Six of the seven reagents showed a significantly different VDA signal when combined with the *NF1* shRNA **(Fig. 3A)**.

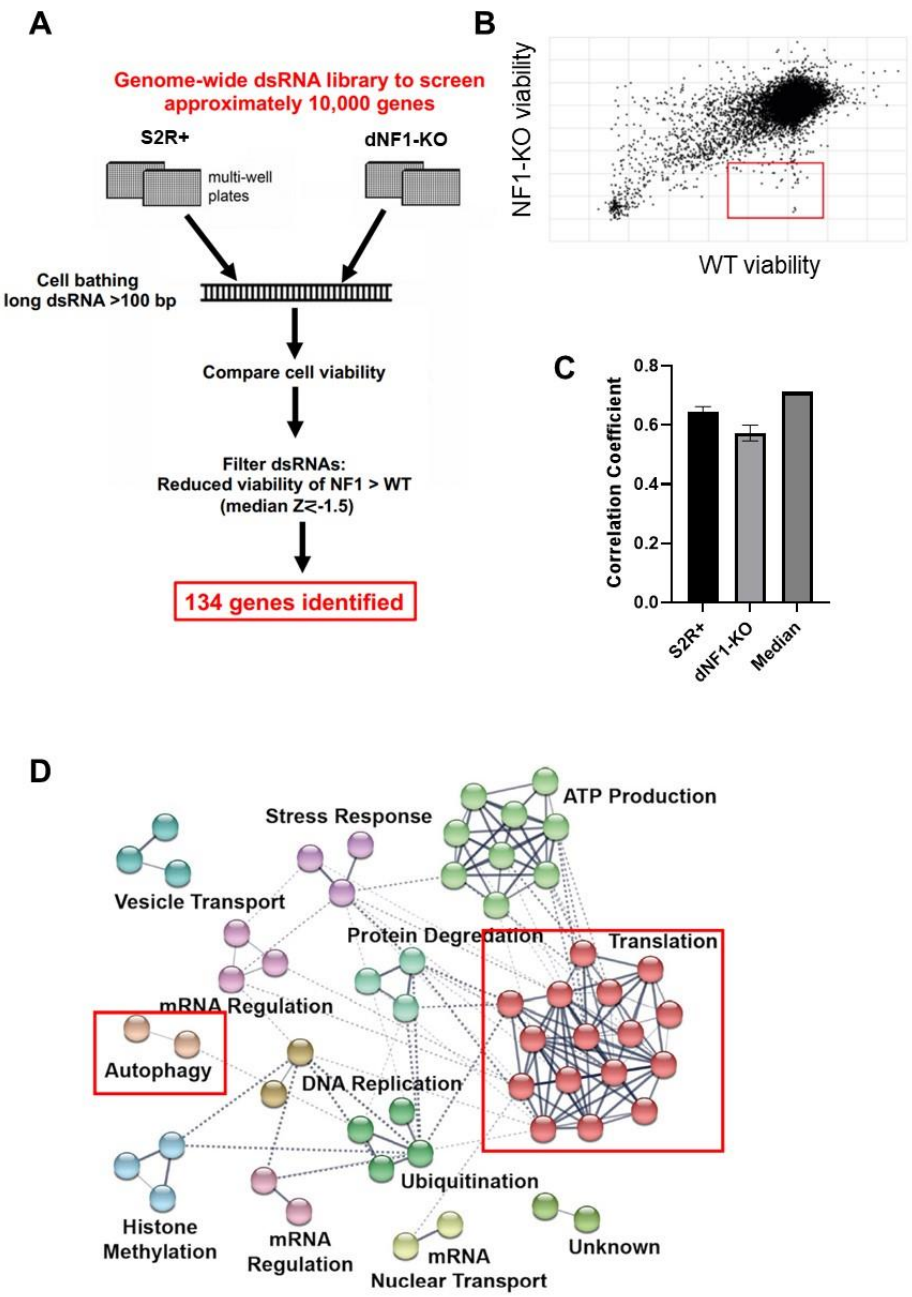

Figure 2. A network of synthetic lethal interaction for *Drosophila* NF1.

(A) Using the NF1-KO cells, we used a genome-wide dsRNA library to screen approximately 10000 genes, resulting in 134 genes identified as having a synthetic lethal interaction with *NF1*. **(B)** Summary of results from the synthetic lethal screen. Z-scores are plotted for NF1-KO cells on the vertical axis and WT S2R+ cells on the horizontal axis. The red box indicates the position of reagents selected as hits. **(C)** Correlation analysis of screen replicates indicating high data quality. Each bar represents the correlation coefficient from comparison between two screen replicates in WT or NF1-KO cells as indicated or between the median Z-scores for each cell line. **(D)** A synthetic lethal interaction network for *NF1*. Solid lines represent physical interactions within functional groups and dashed lines represent physical interactions between functional groups.

Table 1. Selected top ranked hits from screens for NF1 synthetic lethal interactors

Gene Symbol	FBgn ID	Human ortholog	Delta-Z	Function
CG10516	FBgn0036549	SPSB3	3.74	Protein degradation (inferred)
RpL13A	FBgn0037351	RPL13A	3.3	Protein translation
Atg8b	FBgn0038539	GABARAP	2.6	Autophagy
eIF3i	FBgn0015834	EIF3I	2.04	Protein translation
Rpt3R	FBgn0037742	PSMC4	1.87	Proteosome regulation
Rbbp5	FBgn0036973	RBBP5	1.85	Histone methylation
RpS6	FBgn0261592	RPS6	1.79	Protein translation
Uba1	FBgn0023143	UBA1	1.76	Ubiquitination
RpL34a	FBgn0039406	RPL34	1.69	Protein translation
geminin	FBgn0033081	GMNN	1.55	DNA replication

We then used the VDA assay as an additional combinatorial screen to assess synthetic lethality between *NF1* and all 54 candidate drug targets. Two shRNAs targeting each of the genes were generated. These reagents were tested in S2R+ and dNF1-KO cells. Of the 54 genes, 46 showed a >10% reduction in viability in dNF1-KO cells compared to S2R+ controls (**Fig. 3B**; ranked in order of effect on dNF1-KO viability). These results indicate that the network is a reliable representation of the synthetic lethal interaction profile of the *NF1* gene.

In order to identify potential drugs for repurposing to treat NF1 tumours, we filtered the candidate gene list to those that could be targeted by existing drugs. This resulted in eight candidate drugs targets (**Fig. 3C**). We then removed candidates that had previously been studied in relation to NF1, leaving six (including MEK as a control) candidate drug targets (**Table 2**), most of which were FDA-approved. Note that two drugs were included targeting autophagy, resulting in seven candidate drugs.

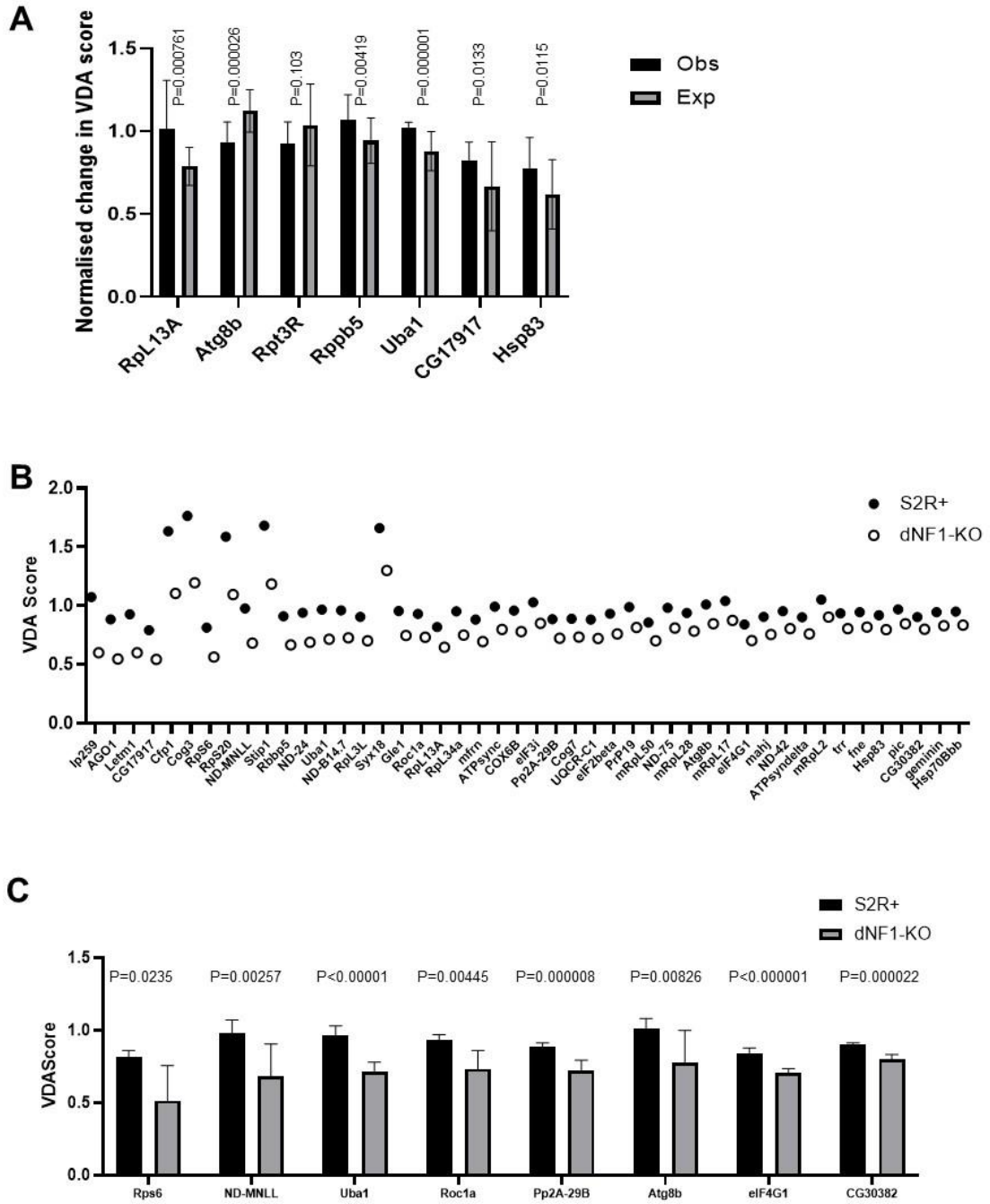

Figure 3. Additional screening of candidate drug targets using VDA analysis.

(A) Validation of the interactions between the indicated genes and NF1 using VDA assays. Bars indicate the average of at least 17 replicates (RpL13A: Obs n=24; Exp n=24, Atg8b: Obs n=22; Exp n=17, Rpt3R: Obs n=18; Exp n=18, Rbbp5: Obs n=24; Exp n=24, Uba1: Obs n=24; Exp n=24, CG17917: Obs n=24; Exp n=24, Hsp83: Obs n=24; Exp n=24; error bars indicate SD; P values calculated using two-tailed t-tests comparing observed and expected values). **(B)** VDA assays performed for all 54 candidate genes, with two shRNAs per gene, in WT S2R+ (black) and dNF1-KO (white) cells. Shown is the best shRNA from the 46 genes that reduced dNF1-KO viability by >10% relative to S2R+ controls ranked in order of effect. **(C)** shRNA gene knockdowns that resulted in a >10% reduction in dNF1-KO viability

compared to S2R+ controls and were druggable targets. Bars indicate the average of nine biological replicates and error bars indicate SD. All eight showed a significant reduction in dNF1-KO viability relative to WT controls assessed using two-tailed, unpaired t-tests.

Table 2. Candidate genes that decreased dNF1-KO viability and were druggable targets without previous evidence of an interaction with NF1

Drug	Target: DM (Human)
Chloroquine*	Atg8b (GABARAP), RpS6 (RPS6)
EAD1	Atg8b (GABARAP), RpS6 (RPS6)
Selumetinib*	Dsor1 (MEK, MAPKK)
Metformin*	ND-MNLL (NDUFB1)
PYR41	Uba1 (UBA1)
LB100	Pp2A-29B (PPP2R1A and PPP2R1B)
Bafilomycin A1	Atg8b (GABARAP), RpS6 (RPS6)

*FDA-approved

Inhibitors selectively affect NF1-deficient *Drosophila* and human cells

Repurposing existing drugs represents the most efficient route to develop new therapeutics. Each of the seven drugs that target the *NF1* synthetic lethal partner genes were first tested in S2R+ and dNF1-KO cells using CellTiter-Glo assays to measure the viability after 48 h of treatment (**Fig. S2)**. Of the seven drugs tested in DM cells, we selected the two autophagy inhibitors (CQ and bafilomycin A1) for further study in human *NF1* mutant cells, as both showed a significant and consistent effect on reducing dNF1-KO viability.

Autophagy inhibitors selectively affect NF1-deficient Drosophila and human cells

One of the strongest hits from the screen was *Atg8b*, which encodes a key component of the autophagy pathway. Autophagy is commonly inhibited experimentally using CQ, which is clinically used as an anti-malarial and shows anti-viral properties, and bafilomycin A1. CQ functions to inhibit autophagy by blocking the binding of autophagosomes to lysosomes by diffusing into the lysosomes and altering the acidic environment, thereby inhibiting autophagic lysosomal degradation [20]. On the other hand, bafilomycin A1 disrupts autophagic flux by independently inhibiting V-ATPase-dependent acidification and Ca-P60A/SERCA-dependent autophagosome-lysosome fusion [21]. We focused on CQ because it is generally well tolerated and can inhibit autophagy *in vivo* at clinically achievable concentrations [22], and bafilomycin A1 because it is a potent inhibitor of autophagy [23].

Firstly, we observed a significant decrease in the baseline autophagy levels of dNF1-KO cells under serum free conditions, with a further increase in the accumulation of autophagic vacuoles when dNF1-KO cells were treated with CQ and bafilomycin A1 (**Fig. 4A**), consistent with inhibition of autophagy**.** We then tested whether CQ and bafilomycin A1 would phenocopy the selective effect observed using genetic inhibition of *Atg8b* in *Drosophila* cells. Both S2R+ and dNF1-KO cells were treated with varying doses of CQ or bafilomycin A1 and cell viability was measured using CellTiter-Glo assays, PI staining, and annexin V staining. A significantly greater effect on dNF1-KO cell viability was observed at multiple concentrations of each drug in serum free media after 48 h of treatment across all three assays, further validating the interaction between autophagy and NF1 and demonstrating that the effect is cytotoxic (**Fig. 4B-F**).

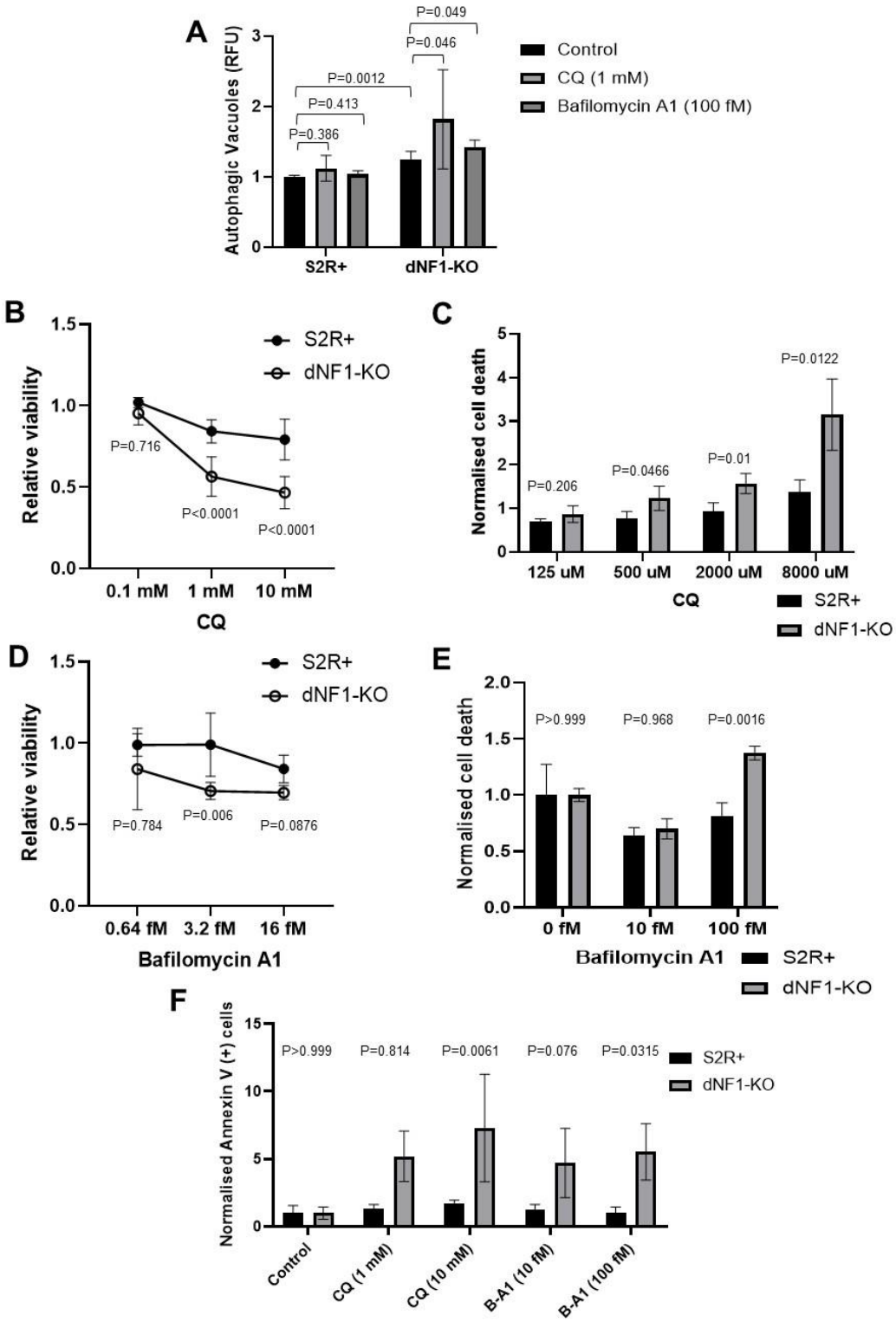

Figure 4. CQ and bafilomycin A1 selectively affect NF1-deficient *Drosophila* cells.

(A) In comparison the S2R+ control cells, we observed a significant increase in autophagy in dNF1-KO cells. Furthermore, CQ (1 mM, 48 h) and bafilomycin A1 (100 fM) selectively increased the accumulation of autophagic vacuoles in dNF1-KO cells (n=9; P values obtained using a two-way ANOVA with Tukey for multiple comparisons). **(B)** CQ reduced dNF1-KO cell viability compared to S2R+ cells after 48 h in serum free media using the CellTiter Glo assay (n=16; P values obtained using a two-way ANOVA with

Tukey for multiple comparisons). **(C)** Analysis of cell death using PI staining with CQ in WT and NF1-KO DM cells (n=4; P values obtained using a two-way ANOVA with Tukey for multiple comparisons). **(D)** Bafilomycin A1 reduced dNF1-KO cell viability compared to S2R+ cells after 48 h in serum free media using the CellTiter Glo assay (n=16; P values obtained using a two-way ANOVA with Tukey for multiple comparisons). **(E)** Analysis of cell death using PI staining with bafilomycin A1 in WT and NF1-KO DM cells (n=4; P values obtained using a two-way ANOVA with Tukey for multiple comparisons). **(F)** CQ and bafilomycin A1 (B-A1) increased annexin V staining in dNF1-KO cells relative to S2R+ controls after 48 h in serum free media (n=6; P values obtained using a two-way ANOVA with Tukey for multiple comparisons). In all cases, data represent the mean and error bars indicate SD.

To determine whether the selective effect of CQ and bafilomycin A1 was conserved in human cells, we tested the effects of drug treatment on a panel of human *NF1* mutant cell lines. These included CRISPR/Cas9-generated C8 *NF1*$^{+/-}$ and C23 *NF1*$^{-/-}$ immortalized Schwann cells [unpublished data] and two pairs of immortalized Schwann cells (pair 1: ipnNF95.11C (*NF1*$^{+/-}$*)* and ipNF95.11b 'C' (*NF1*$^{-/-}$*)*, pair 2: ipnNF09.4 (*NF1*$^{+/-}$*)* and ipNF05.5 (*NF1*$^{-/-}$*)*) derived from plexiform neurofibromas [24]. Baseline autophagy levels were found to be significantly higher in C23 and ipNF05.5 *NF1*$^{-/-}$ cells relative to C8 and ipnNF09.4 *NF1*$^{+/-}$ controls, with the opposite observed in ipNF95.11b 'C' cells (**Fig. 5A-C**). CQ increased the accumulation of autophagic vacuoles in all *NF1*$^{-/-}$ cells, but not *NF1*$^{+/-}$ controls. However, bafilomycin A1 only increased the accumulation of autophagic vacuoles in the patient *NF1*$^{-/-}$ cells and not the C23 cells. Both CQ and bafilomycin A1 resulted in a significantly greater reduction in the viability of homozygous *NF1*$^{-/-}$ mutant cells compared to heterozygous *NF1*$^{+/-}$ controls after 48 h of treatment under serum free media conditions, as measured with the CellTiter-Glo and caspase assays (**Fig. 5D-L**). This suggests that there may be differences in mechanism between cell models although the selective viability effect is consistent.

Together, these results demonstrate that NF1-deficient cells have vulnerability to disruption of the autophagy pathway that is conserved and reproducible between *Drosophila* and human Schwann cells derived from NF1-associated tumours. Not only does autophagy represent a promising pathway for exploiting for the potential treatment of NF1-associated tumours, but we identified CQ and bafilomycin A1 as candidate drugs for the treatment of NF1 tumours.

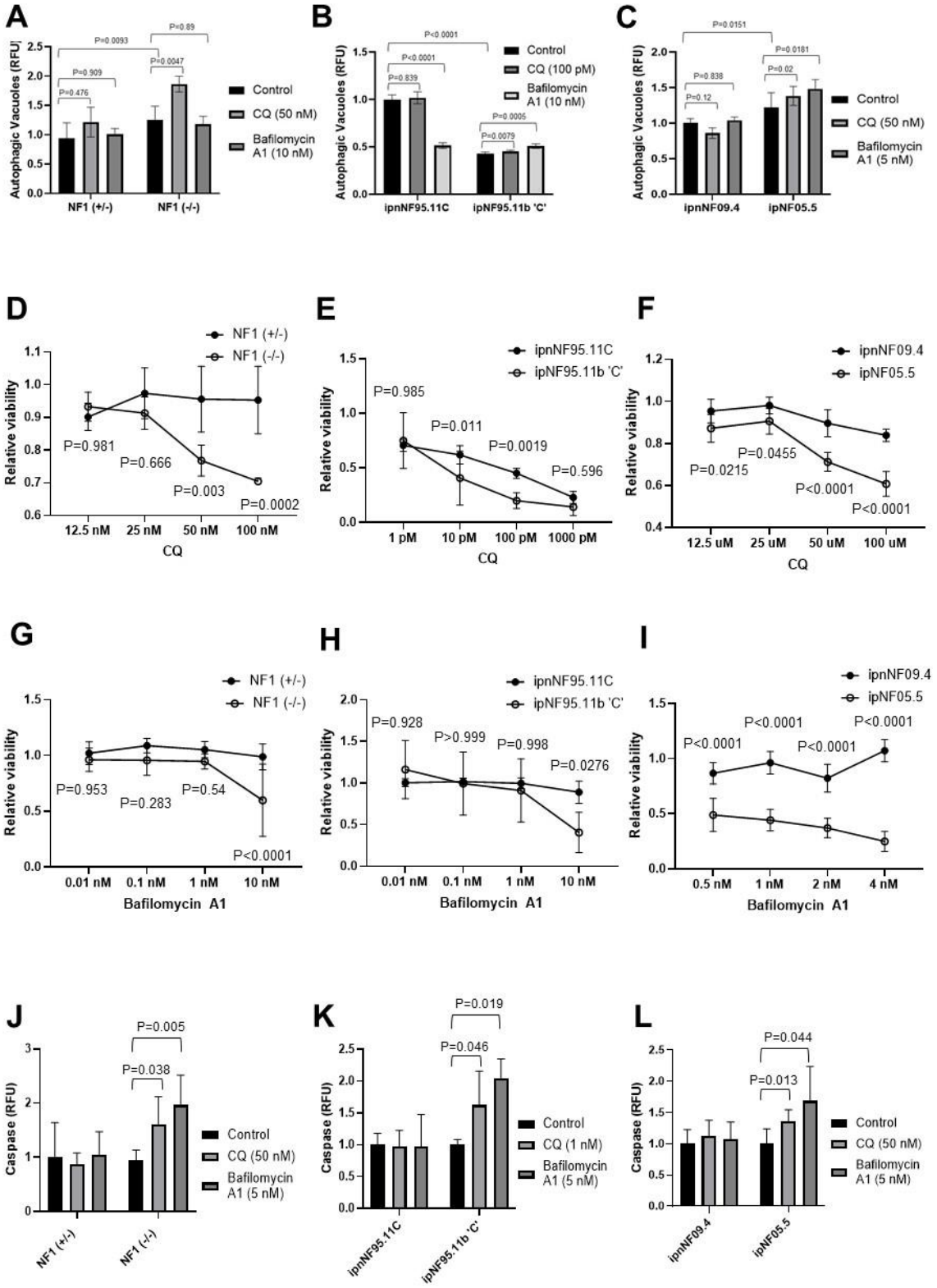

Figure 5. CQ and Bafilomycin A1 selectively affect NF1-deficient human cells.

CQ (50 nM) increased the accumulation of autophagic vacuoles in C23 *NF1*$^{-/-}$ cells but not in C8 *NF1*$^{+/-}$ controls **(A)**, in ipNF95.11b 'C' *NF1*$^{-/-}$ cells but not in ipnNF195.11C *NF1*$^{+/-}$ controls **(B)**, and in ipNF05.5 *NF1*$^{-/-}$ cells but not in ipnNF04.9 *NF1*$^{+/-}$ controls **(C)** after 48 h in serum free media. However, bafilomycin A1 only increased the accumulation of autophagic vacuoles in the two patient cell lines **(B & C)** (n=9; P

values obtained using a two-way ANOVA with Tukey for multiple comparisons). In addition, we observed an increase in autophagic vacuoles in untreated C23 *NF1*$^{-/-}$ cells and ipNF95.11b 'C' *NF1*$^{-/-}$ cells in comparison to *NF1*$^{+/-}$ controls. CQ significantly reduced *NF1*$^{-/-}$ cell viability relative to *NF1*$^{+/-}$ controls at varying doses in C8/C23 cells **(D)**, ipnNF95.11C/ipNF95.11b 'C' cells **(E)**, and ipnNF09.4/ipNF05.5 cells **(F)** after 48 h in serum free media as measured with the CellTiter Glo assay (n=10-16; P values obtained using a two-way ANOVA with Tukey for multiple comparisons). **(G-I)** Bafilomycin A1 significantly reduced *NF1*$^{-/-}$ cell viability relative to *NF1*$^{+/-}$ controls at varying doses in C8/C23 cells **(G)**, ipnNF95.11C/ipNF95.11b 'C' cells **(H)**, and ipnNF09.4/ipNF05.5 cells **(I)** after 48 h in serum free media as measured with the CellTiter Glo assay (n=10-16; P values obtained using a two-way ANOVA with Tukey for multiple comparisons). We observed an increase in caspase activation in *NF1*$^{-/-}$ cells treated with CQ and bafilomycin A1 (B-A1) for 48 h in serum free media relative to *NF1*$^{+/-}$ controls in C8/C23 cells **(J)**, ipnNF95.11C/ipNF95.11b 'C' cells **(K)**, and ipnNF09.4/ipNF05.5 cells **(L)** (n=9; P values obtained using a two-way ANOVA with Tukey for multiple comparisons). In all cases, data represent the mean and error bars indicate SD.

CQ affects survival in a *Drosophila in vivo NF1* mutant model

As CQ is FDA-approved, well tolerated, and showed a significant effect on dNF1-KO cell viability, we chose to take this drug forward to determine synthetic lethality *in vivo*. *Drosophila* mutant flies show defective Ras signalling, which results in several neurobehavioral phenotypes [25, 26, 27, 28, 29]. For this study, we generated novel *dNf1* null mutant flies using CRISPR gene editing: *dNf1*^{C1} (*dNF1* delAT162-163) and *dNf1*^{C2} (*dNF1* indel (3bp del/7bp insertion) (**Fig. 6A**). Western blots using lysates prepared from adult heads from CRISPR mutants showed no expression of NF1 (**Fig. 6B**). In addition, ELISAs showed a 4-fold increase in pERK/ERK of *dNf1* mutants compared to WT flies (**Fig. 6C**).

To determine whether CQ affects survival in *dNf1* mutant *Drosophila*, we took two approaches. Firstly, we tested flies with pan-neuronal RNAi knock down of dNf1 (using *nSyb-Gal4*) compared to landing site controls on food containing CQ (35 mM). Secondly, we compared the effect of CQ (35 mM) on *dNf1*^{C1}/*dNf1*^{C2} null mutant flies, the WT parental line (control), and *dNf1*^{C1}/*dNf1*^{C2} + *nSyb-Gal4>UAS-dNf1* (re-expression of dNf1 from a *UAS-dNF1* transgene driven with a pan-neuronal (*nSyb-Gal4*) driver). In flies with dNf1 RNAi knockdown, CQ significantly reduced the survival time compared to CQ-treated landing site control flies, and untreated flies (**Fig. 6D**). Similarly, CQ resulted in increased lethality of *dNf1*^{C1}/*dNf1*^{C2} mutants compared to the WT parental line. Furthermore, we were able to rescue the CQ sensitivity of *dNf1* mutant flies by re-expression of dNf1 from a *UAS-dNF1* transgene (**Fig. 6E**). Together, these results demonstrate that *dNf1* mutant flies have vulnerability to disruption of the autophagy pathway, as shown to be conserved and reproducible in *Drosophila* NF1-KO cells

and human Schwann cells derived from NF1-associated tumours. This further highlights the autophagy pathway as a target for the potential treatment of NF1-associated tumours, with CQ as a candidate drug.

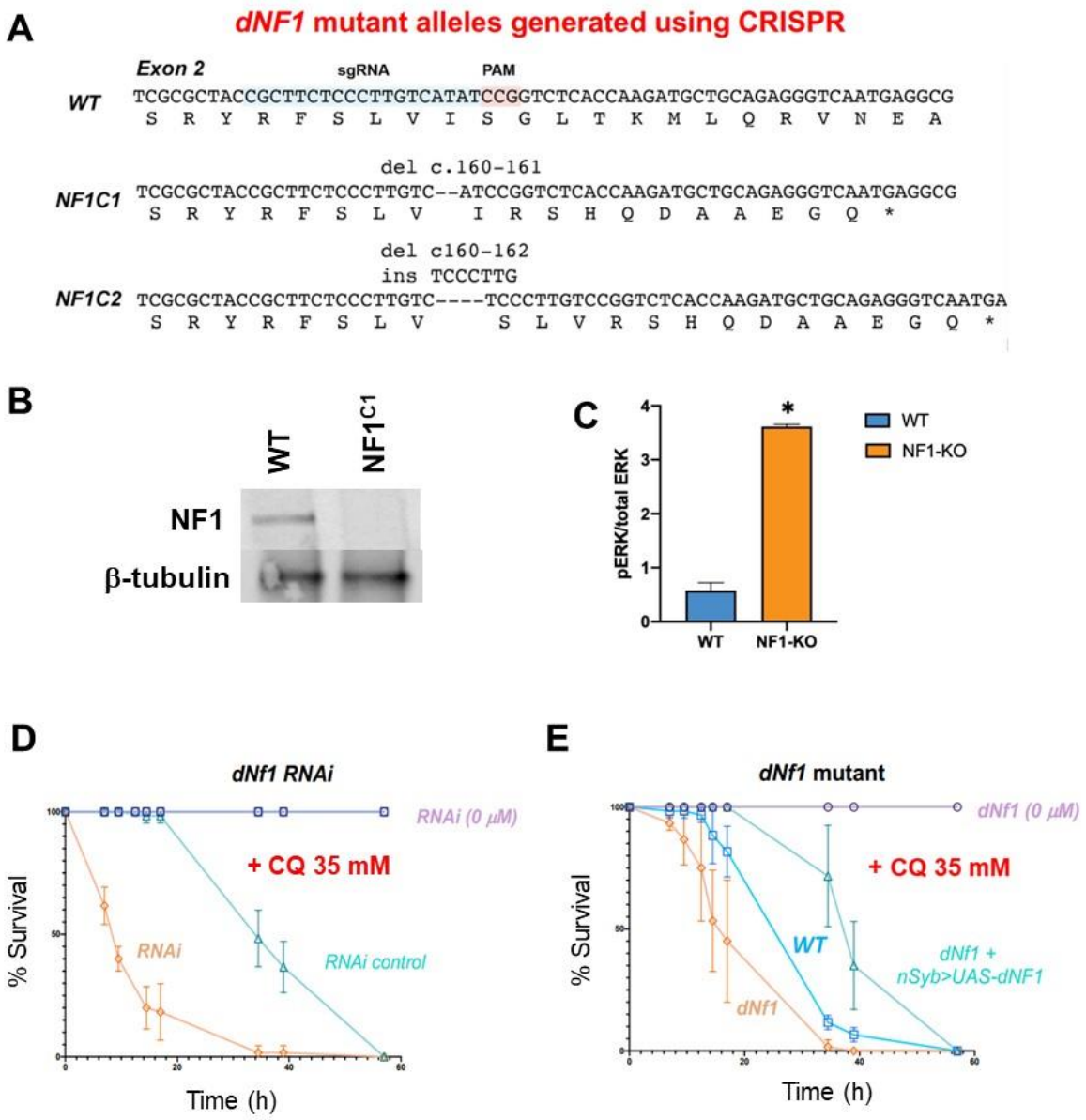

Figure 6. CQ affects lethality in *dNF1* mutant *Drosophila in vivo.*

(A) We generated novel *dNf1* null mutants using CRISPR gene editing: *dNf1*^{C1} (*dNF1* delAT162-163) and *dNf1*^{C2} (*dNF1* indel (3bp del/7bp insertion). **(B)** Western blots of anti-dNf1 immunoprecipitates from lysates prepared from adult heads from CRISPR mutants showed no expression of neurofibromin. **(C)** ELISA for pERK/ERK showed a 4-fold increase in pERK/ERK of *dNf1* mutants compared to WT flies. Error bars indicate the standard deviation between duplicate samples. A paired, two-tailed t-test was performed to determine significance; *P < 0.05. **(D)** In RNAi dNf1 mutant flies, CQ significantly reduced the survival time compared to CQ-treated RNAi control flies, and untreated flies. **(E)** CQ resulted in increased lethality of *dNf1*^{C1}/*dNf1*^{C2} mutants compared to WT flies. We were able to rescue the sensitivity of *dNF1* mutant flies to CQ by re-expression of dNf1 from a *UAS-dNF1* transgene.

Selumetinib enhances to viability effect of CQ and bafilomycin A1

Selumetinib, a MEK1/2 inhibitor, is currently the only FDA-approved drug for the treatment of tumours associated with neurofibromatosis [30]. We treated S2R+ and dNF1-KO cells with selumetinib (10 µM) +/- CQ (1 mM) or bafilomycin A1 (100 pM) for 48 h in serum free media and performed CellTiter-Glo assays to measure cell viability (**Fig. 7A**). When selumetinib was combined with CQ and bafilomycin A1, we saw a further reduction in dNF1-KO, but not S2R+, viability relative to the CQ/bafilomycin A1 only dNF1-KO cells, indicating that selumetinib enhances the effects of CQ/bafilomycin A1 on dNF1-KO cell viability.

Similarly, in C8/C23, ipnNF9511.C/ipNF95.11b 'C', and ipnNF09.4/ipNF05.5 cell lines, selumetinib significantly enhanced the reduced viability effect of CQ in $NF1^{-/-}$, but not $NF1^{+/-}$ cells. Therefore, combined treatment of CQ and selumetinib had a greater impact in NF1-deficient cell viability compared to either drug alone (**Fig. 7B-D**). In addition, selumetinib significantly enhanced the reduced viability effect of bafilomycin A1 in patient $NF1^{-/-}$, but not $NF1^{+/-}$ cells, although not in C23 cells.

The coefficient of drug interaction (CDI) was calculated each cell line treated with CQ + selumetinib or bafilomycin A1 + selumetinib. A CDI<1 indicates synergy, CDI=1 indicates additivity, and CDI>1 indicates antagonism. We observed a fairly strong synergistic effect of CQ + selumetinib in C23 and ipNF05.5 cells, and of bafilomycin A1 + selumetinib in ipNF05.5 cells (**Fig. 7E**).

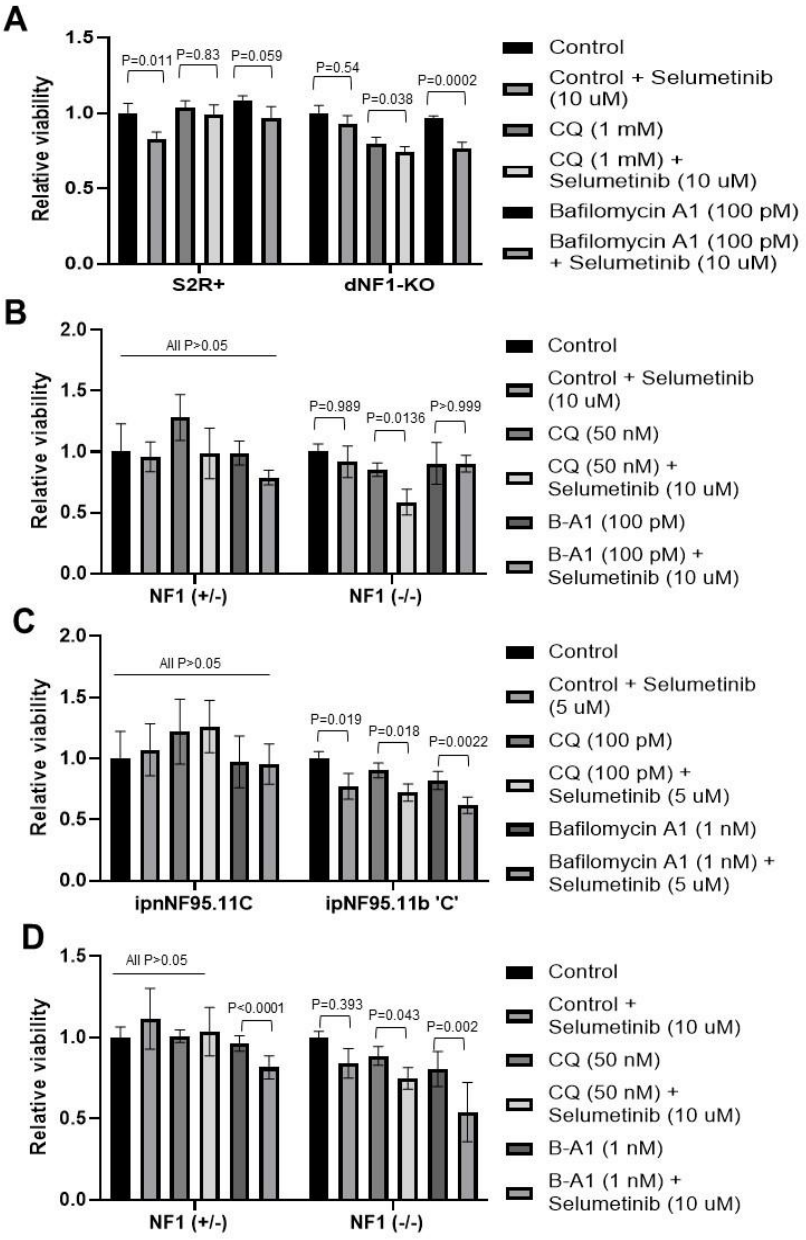

E

Drug synergy	**CDI: CQ + Selumetinib**	**CDI: Bafilomycin A1 + Selumetinib**
dNF1-KO	0.99	0.99
C23	0.72	0.94
ipNF95.11b 'C'	1.0	0.96
ipNF05.5	0.93	0.75

Figure 7. Combined effect of selumetinib with CQ and bafilomycin A1 on cell viability.

(A) S2R+ and dNF1-KO cells were treated with 0 µM or 10 µM selumetinib combined with CQ (1 mM) or bafilomycin A1 (10 pM). Alone, selumetinib significantly reduced the viability of S2R+ but not dNF1-KO cells after 48 h in serum free media, as measured using the CellTiter Glo assay. In combination with CQ or bafilomycin A1, selumetinib resulted in a significantly greater reduction in dNF1-KO cell viability compared to CQ alone, which was not observed in S2R+ cells (n=9; P values obtained using a two-way ANOVA with Tukey for multiple comparisons). **(B)** In a similar experiment in the human cell

lines, selumetinib alone had no effect on C8, C23, ipnNF95.11C, ipnNF09.4, and ipNF05.5 viability **(B-D)**; however, it did significantly decrease ipNF95.11b 'C' *NF1*$^{-/-}$ viability **(C)**. Similar to observations in DM cells, the effect of CQ was enhanced when combined with selumetinib in all three *NF1*$^{-/-}$ cell lines, whereas the effect of bafilomycin A1 was enhanced by selumetinib only in the patient NF1-deficient cell lines (ipNF95.11b 'C' and ipNF05.5). (n=9; P values obtained using a two-way ANOVA with Tukey for multiple comparisons). In all cases, data represent the mean and error bars indicate SD. **(E)** Drug synergy between CQ + selumetinib and bafilomycin A1 + selumetinib was calculated using the coefficient of drug interaction (CDI). CDI<1 indicates synergism, CDI=1 indicates additivity, and CDI>1 indicates antagonism.

DISCUSSION

Using dNF1-KO cells as a model, we applied the method of synthetic lethal screening to identify candidate drug targets to treat NF1-deficient tumours. We further validated the 54 candidate synthetic lethal partner genes to NF1 using VDA as an additional combinatorial screening method and prioritised those that could be targeted with existing drugs. This resulted in a list of eight candidate genes that resulted in a >10% decrease in dNF1-KO viability and were druggable targets. After further filtering of these targets to select those not previously identified as having a lethal interaction with NF1, we screened seven existing drugs targeting six candidate genes in dNF1-KO and S2R+ cells, noting that the autophagy inhibitors CQ and bafilomycin A1 resulted in a significant reduction in dNF1-KO cell viability. Notably, this effect was conserved in a panel of human NF1 mutant cell lines. Finally, we showed that the effect of CQ was conserved in a *Drosophila NF1*-mutant *in vivo* model. The results of this study highlight two key points: 1) the use of *Drosophila* cells as a model to screen for drugs specifically targeting *NF1* mutant cells was highly successful as the candidate interactions were conserved across a panel of human *NF1* mutant cells and an *in vivo* fly *NF1* mutant model, and 2) NF1-deficient cells have vulnerability to disruption of the autophagy pathway. Not only does this pathway represent a promising target for the treatment of NF1-associated tumours, but we identified CQ and bafilomycin A1 as candidate drugs for the treatment of NF1 tumours.

We have previously reported the success of a synthetic screening method similar to the one used in this study, which combines CRISPR genome editing with RNAi [13, 14]. This approach has several advantages over the use of multiple RNAi reagents to perform combinatorial screens in *Drosophila* cells, including a reduction in the noise associated with dual RNAi screening, a homogenous population of null mutants, and in-depth characterisation of the

mutant cell line prior to screening. Furthermore, previous screening methods have required a laborious secondary screen and further validation of candidate genes; however, using the CRISPR-RNAi combinatorial screening method in the present study, we could quickly identify the most robust candidates, which is reflected in the fact that we validated 86% of our candidate genes using VDA. In addition, we validated two of the most effective drugs (CQ and bafilomycin A1) through to a panel of mammalian cell models of NF1. Therefore, screening in *Drosophila* cells as a model organism was rapidly translated to the identification of clinically relevant potential drugs, as shown previously [14]. Finally, by performing the screen in *Drosophila* cells, this increases the likelihood of reproducible effects in mammalian models.

We identified *Atg8b* as a synthetic lethal partner to *NF1* in the genome-wide synthetic lethal screen, which was then validated in the VDA combinatorial screen. Atg8b (human ortholog: GABARAP) is an autophagy-related gene located in the autophagosome. Autophagy is the process where damaged organelles and unfolded proteins are sequestered into autophagosomes in the cytoplasm, which then undergo fusion with lysosomes (autolysosomes) resulting in degradation of the intracellular components [31]. This is important in the regulation of cell growth, maturation, and death. In cancer, autophagy is reported to take on two roles: 1) degradation of damaged organelles and recycling of macromolecules to maintain a stable cellular environment, which prevents the formation of tumours [32]; and 2) aiding in cancer cell survival in response to growth-limiting conditions, contributing to tumorigenesis [33]. Furthermore, autophagy has been widely reported to promote cancer cell survival through a drug resistance mechanism [33, 34]. Therefore, targeting the autophagy pathway is a potential therapeutic option in the treatment of cancer.

As *Atg8b* was found to be a consistent and reproducible synthetic lethal partner gene to NF1, we hypothesized that inhibition of autophagy would have a similar lethal effect on NF1-deficient cell viability. The first inhibitor, CQ, is a widely used anti-malarial that functions to inhibit autophagy by blocking the binding of autophagosomes to lysosomes by diffusing into the lysosomes and altering the acidic environment, thereby inhibiting autophagic lysosomal degradation [20]. Previous studies have shown that CQ has anti-tumour properties in several types of cancer, including glioblastoma [35, 36], hepatocellular carcinoma [37], prostate cancer [38], breast cancer [39], and pancreatic cancer [40]. Similarly, we found that CQ significantly reduced dNF1-KO cell viability relative to S2R+ cells across a range of concentrations under conditions where autophagy is induced (serum starvation of cells and NF1 deficiency). This effect of CQ was conserved across a panel of three human NF1-deficient cell lines, two of which were derived from patient neurofibromas, as well as in an *in vivo* fly model of deficient NF1. Therefore, CQ shows great potential as an anti-tumour therapy in NF1-associated tumours.

However, whilst there is a vast array of evidence for the efficacy and safety of CQ, the underlying mechanisms of the tumour suppressive actions of CQ remain to be determined. One potential mechanism is that under starvation conditions, such as those used in this study, a reduction in glucose transport results in a release of mTOR inhibition of the ULK1 complex, inducing vesicle nucleation and facilitating the process of autophagy. Inhibition of the lysosome using CQ has been shown inhibit tumour growth and induce tumour cell death *in vitro* [41, 42]. However, why is it that NF1 mutant cells are more susceptible to autophagy inhibition with CQ? RAS has previously been shown to regulate autophagic flux [43]. In addition, cancers associated with RAS mutations have been reported to be dependent on autophagy, although this appears to be tumour cell line dependent [44, 45]. Therefore, cancers with aberrant RAS activity can be more susceptible to autophagy inhibition with CQ.

The second autophagy inhibitor that we screened was bafilomycin A1, a macrolide antibiotic that disrupts autophagic flux by independently inhibiting V-ATPase-dependent acidification and Ca-P60A/SERCA-dependent autophagosome-lysosome fusion [21]. Although some studies have shown bafilomycin A1 to promote cancer cell apoptosis, its toxicity potential has limited its medical applications [22]. We found that bafilomycin A1 selectively reduced dNF1-KO cell viability relative to S2R+ controls at very low concentrations (0.1 fM – 3.2 fM), with little effect on S2R+ cell viability. This effect was also conserved in the panel of three human NF1-deficient cell lines at concentrations <10 nM. Similar results have been observed in paediatric B-cell lymphoblastic leukaemia cells [46] and pancreatic cancer cells [47]. Regarding the mechanism of bafilomycin A1, it has been reported to inhibit both late-stage autophagy and early-stage autophagy by activating mTOR and attenuating formation of the Beclin 1-Vps34 complex [46].

Ras signalling is implicated in autophagy regulation. NF1 functions as a RasGAP (GTPase-activating protein), which facilitates Ras inactivation by enabling its GTPase activity [48]. In NF1-associated tumours, NF1 expression is downregulated, resulting in aberrant Ras activity and upregulation of the PI3K/Akt/mTOR1 pathway. Therefore, aberrant Ras activity is expected to negatively regulate autophagy; however, Ras is implicated in many signalling pathways and so it has a multifaceted role in autophagy regulation. For example, Ras also activates the Raf-1/MEK1/2/ERK and Rac1/MKK7/JNK signalling pathways, both of which are known to activate autophagy [43]. Therefore, we speculate that aberrant Ras activity in NF1-deficient cells results in the initiation of autophagy, and that inhibition of this pathway has anti-tumour effects. When combining our data on the effects of CQ and bafilomycin A1, we provide strong evidence for inhibition of the autophagy pathway as a target in the treatment of NF1-associated tumours.

Furthermore, inhibition of autophagy with CQ and bafilomycin A1 increased the sensitivity of NF1-deficient cells (both dNF1-KO and human NF1$^{-/-}$ cells) to MEK1/2 inhibition with selumetinib. Selumetinib is currently the only FDA-approved drug for the treatment of tumours associated with neurofibromatosis [30]. The phase 2 trial (SPRINT) for the use of selumetinib in plexiform neurofibromas reported clinically meaningful improvements in 71% of patients [7], prompting its FDA approval for patients ages 2 to 18 years with neurofibromatosis type I who have symptomatic, inoperable plexiform neurofibromas. However, there are some toxicity effects related to long-term MEK inhibition [7]. Our data implies that autophagy inhibition via CQ or bafilomycin A1 could be an effective adjunctive therapy for NF1-associated tumours. This is in line with a previous study, which showed that combined inhibition of MEK1/2 plus autophagy had a synergistic anti-proliferative effect in pancreatic ductal adenocarcinoma cell lines, which display aberrant K-Ras activity, as well as patient-derived pancreatic ductal adenocarcinoma xenograft tumours in mice [49].

In conclusion, combinatorial screening in CRISPR-generated dNF1-KO cells with RNAi resulted in the identification of potential candidate drugs for the treatment of NF1-associated tumours, two of which were validated in this study. The conservation of the synthetic lethal interactions between *Drosophila* and human NF1 mutant cells demonstrates the robustness of our combinatorial screening method.

METHODS

Cell culture

Drosophila Schneider (S2R+) cells, both WT and dNF1-KO, were cultured at 25°C in Schneider's media (Gibco) containing 1% antibiotic (Gibco) and 10% fetal bovine serum (Gibco). Human cell lines included *NF1*$^{+/-}$ and *NF1*$^{-/-}$ immortalised human Schwann cell (SC) lines, derived from the 02.3λ cell line from a healthy individual [50] using CRISPR/Cas9 gene editing to introduce *NF1* indels; *NF1*$^{-/-}$ CRISPR SCs have been shown to have *in vivo* tumourigenic potential in mice (unpublished data). In addition, we used two immortalised human SCs derived from plexiform neurofibromas from NF1 patients [24], which included ipnNF95.11C (*NF*$^{+/-}$) and ipNF95.11b'C' (*NF1*$^{-/-}$) cells (germline *NF1* mutation: c.1756delACTA), and ipNF09.4 (*NF1*$^{+/-}$) and ipNF05.5 (*NF1*$^{-/-}$) cells (germline *NF1* mutation: c.3456_3457insA). All human cell lines were cultured at 37℃ in 5% CO_2 in DMEM media (Merck) containing 1% antibiotic (Gibco) and 10% fetal bovine serum (Gibco). For ipnNF09.4 and ipNF05.5 cells, the media was also supplemented with 50 ng/ml neuregulin-1 (NRG-1) (Sigma).

Generation of NF1-KO *Drosophila* cells

The dNF1-KO cell line was generated as described previously [14, 16]. Wild-type S2R+ cells were co-transfected with the pl018 plasmid to express Cas9 and the sgRNA (CGCTTCTCCCTTGTCATATC) and pAct-GFP plasmid to mark transfected cells. Five days after transfection, individual cells with the highest 15% GFP signal were isolated and seeded into wells of 96-well plates using FACS. Single cells were cultured using conditioned media for approximately 3 weeks. DNA was then extracted from each candidate cell population and assessed using HRMA to identify those carrying mutations at the sgRNA target site. Positive candidates were then sequenced to confirm homozygous frame-shift mutations were present (**Fig. 1A**).

Synthetic lethal screen

Screens were performed using WT S2R+ or dNF1-KO cells as described previously using the genome-wide RNAi library from the Sheffield RNAi Screening Facility (SRSF). In total, 10,000 cells were seeded into each library well in 10 µl serum free Schneider's *Drosophila* media. Plates were then incubated at room temperature for 45 minutes before addition of 35 µl media with 10% FBS. Libraries were incubated at 25°C for 5 days before CellTiter-Glo® assays were performed. Screens were performed in triplicate in each cell line.

Data were analysed by first normalising all values to the median of each row and column of the library plate to allow direct comparison between plates. Z-scores were then calculated for each RNAi reagent using the average and standard deviation of each replicate screen. Reagents were considered hits if the Z-score in at least 2/3 of replicates was below -1.5 in NF1-KO cells and above -1.5 in S2R+ cells.

Variable dose analysis (VDA)

VDA is an RNAi-based method in which each cell within a population receives a different dose of shRNA. The relative knockdown efficiency of each cell is then measured with a fluorescent reporter. On the day of transfection S2R+ (WT) and dNF1-KO cells were plated at 1 x 10^4 cell/100 µl culture media, per well of a 96-well plate. Cells were incubated at 25℃ for 40 mins to allow adhesion. Cells were then transfected with 40 ng actin-GFP and 160 ng shRNA expression plasmid using 0.6 µl FuGENE® HD transfection reagent in a total volume of 10 µl . We used a positive (*thread*, an apoptosis inhibitor that induces cell death when inhibited) and negative (*white*, known to have no viability effect in these cells) shRNA on each plate for normalisation of data. Plates were then sealed and incubated for 4 days at 25℃ in a humidifying chamber.

Flow cytometry was used to identify GFP-positive cells (transfection efficiency). A Matlab script was used to determine the area under the curve (AUC), normalised to the positive and negative control, as a measure of transfected cell viability. More detailed protocol and data analysis information can be found in Sierzputowska et al. [51].

CellTiter-Glo® assays

The CellTiter-Glo® assay (Promega; G7570) is a luminescent viability assay based on the quantification of ATP, which is an indicator of metabolically active cells. All cells were plated in white 384-well plates at a seeding density of 5 x 10^3 cells/25 µl culture media in either complete or serum free (SF) media. S2R+ cells were left to adhere for 40 mins at 25℃ and human cells were left to adhere for 4 h at 37℃ in 5% CO_2 before treatment. Cells were treated with 250 nl per well of each drug (CQ, bafilomycin A1, and selumetinib) in PBS at varying concentrations in replicates of 5-8 using the Mosquito LV Genomics (SPT Labtech) and incubated for 48 h. The CellTiter-Glo® assay was then performed according to the manufacturer's instructions, and luminescence was measured using a plate reader (TECAN Infinite M200 Pro).

Autophagy assay and Caspase assay

An autophagy assay kit (abcam; ab139484) was used to measure autophagic vacuoles in live cells using a dye that selectively labels autophagic vacuoles. All cells were plated in 96-well plates in either complete or serum free (SF) media. S2R+ cells were left to adhere for 40 mins at 25℃ and human cells were left to adhere for 4 h at 37℃ in 5% CO_2 before treatment. Cells were treated with 1 µl per well of each drug (CQ, bafilomycin A1) in PBS at varying concentrations in replicates of three, and incubated for 48 h. The autophagy assay was then performed according to the manufacturer's instructions, and fluorescence intensity was measured using a plate reader (TECAN Infinite M200 Pro). Caspase activity was assessed using the same plating and treatment method via the generic caspase activity assay kit (abcam; ab112130) per the manufacturer's instructions. In both the autophagy and caspase assay, autophagy/caspase fluorescence was normalised to dapi in each well.

Annexin V and PI staining

The Annexin V-FITC apoptosis kit (abcam; ab14085) was used to detect apoptosis by staining of phosphatidylserine molecules that have translocated to the outside of the cell membrane. Cells were co-stained with propidium iodide (PI) to detect dead cells in the population. S2R+ cells were left to adhere for 40 mins at 25℃ before treatment. Cells were treated with 1 µl per well of each drug (CQ, bafilomycin A1) in PBS at varying concentrations in replicates of three,

and incubated for 48 h. The annexin-V/PI assay was then performed according to the manufacturer's instructions, and fluorescence intensity was measured using flow cytometry.

Drosophila **husbandry and stocks**

Flies were cultured on cornmeal/agar food medium according to standard protocol and housed at 25°C.

The *Nf1*^{C1} and *Nf1*^{C2} mutant fly lines were generated by CRISPR/Cas9 [52] using the sgRNA line: *y[1] sc[*] v[1] sev[21]; P{y[+t7.7] v[+t1.8]=TKO.GS01796}attP40* (GS01796 sgRNA sequence: CGCTTCTCCCTTGTCATATC) and a germline source of Cas9: *y[1] M{w[+mC]=nos-Cas9.P}ZH-2A w[*]* (Bloomington Stock #54591). The *UAS-dNf1* transgene encodes full-length *dNf1* cDNA corresponding to the RF isoform with the addition of introns 9 and 10 and was previously published [53]. RNAi and landing site control lines were obtained from the Transgenic RNAi Project (TRiP) and Vienna *Drosophila* RNAi Center: *dNf1 RNAi* lines: P{TRiP.JF01866}attP2 JF01866 (Bloomington Stock: 25845), P{KK101909}VIE-260B (VDRC #109637); control crosses consisted of empty attP landing site lines: P{y[+t7.7]=CaryP}attP2 (Bloomington Stock: 36303) and VIE-260B (VDRC #60100). *UAS-dicer2* was included to potentiate the RNAi effect [54]: *P{w[+mC]=UAS-Dcr-2.D}2* and *P{w[+mC]=UAS-Dcr-2.D}10* (Bloomington: 24650 and 24651). Male flies were used for all experiments.

Assessing drug sensitivity in flies

Flies were raised on standard fly food and kept at 25°C. For testing drugs, adult flies were transferred to Formula 4-24 Instant *Drosophila* Medium (Carolina Biological) prepared using water (control) or 35 µM CQ (chloroquine diphosphate; Sigma C6628) in water. For each genotype, three replicates of 20 flies were added to each condition and kept at 25°C. Flies were monitored periodically to assess lethality. Survival was reported as the percent of flies still alive at each time point.

Western blotting

Expression of neurofibromin in S2R+ cells was assessed using western blotting. Lysates were prepared in RIPA buffer and analysed as detailed below. Expression of neurofibromin in adult flies was assessed using immunoprecipitation (IP) followed by western blotting. Lysates of heads from 2 to 3-day old adult flies were prepared using IP buffer (50 mM Tris-HCl pH 7.5, 125 mM NaCl, 1.5 mM MgCl2, 0.2% NP-40, 5% glycerol) supplemented with protease inhibitors (Complete Protease Inhibitor Cocktail, Sigma) and phosphatase inhibitors

(NaF/Na3VO4/β-glycerophosphate). Immunoprecipitations were performed using 400 µg of total protein in 1 ml IP buffer incubated with 200 µl of mAb21 anti-neurofibromin monoclonal antibody supernatant [55] for 1 h at 4°C. Immunocomplexes were precipitated with a mix of Protein A- and Protein G-Sepharose beads (1:1, Sigma) for 1 h at 4°C before washing three times with IP buffer and denaturing with 2× SDS sample buffer. Lysates and immunoprecipitates were resolved on NuPAGE 3–8% Tris-Acetate (for neurofibromin) or NuPAGE 4–12% Bis-Tris gels (pERK/ERK/β-tubulin). After transfer to nitrocellulose membranes, blots were processed according to the Odyssey CLx protocol (LI-COR). Antibodies used for immunoblotting: anti-neurofibromin (mouse, mAb21, 1:10), anti-β-tubulin (mouse, Developmental Studies Hybridoma Bank E7, 1:10,000), anti-mouse IRDye secondary antibody (goat, Invitrogen, A32730, 1:10,000), and anti-rabbit IRDye (donkey, Invitrogen, A10043, 1:10,000) secondary antibody.

ELISA

pERK/ERK levels were assessed using the ERK1/2 (pT202/Y204) + ERK1/2 Total SimpleStep ELISA Kit from Abcam (ab176660). Briefly, 20 *Drosophila* heads were lysed in 60 µL of Cell Extraction Buffer with Enhancer in 1.5 mL Eppendorf tubes with a pestle to yield a protein concentration of 10 µg/µL. Lysates were spun for 5 mins at 13k rpm at 4ºC and transferred to new tubes and diluted to 0.5 µg/µL (12.5 µL of lysate plus 237.5 µL of buffer). Each sample was run in duplicate using 50 µL of diluted protein for a total of 25 µg per sample. Samples were incubated with either p-ERK1/2 or total ERK1/2 antibody cocktail for 1 h at room temperature with agitation prior to colour development driven by the addition of TMB substrate. After adding the stop solution, the OD was read at 450 nm using a SpectraMax Plus microplate reader. The pERK/total ERK ratio was determined by dividing the pERK reading by the total ERK reading. Error bars represent the SD. A paired, two-tailed t-test was performed to determine significance; *P < 0.05.

ACKNOWLEDGEMENTS

Research support was provided by the Medical Research Council (MR/V009583/1) and the University of Exeter (B.E.H), and NIH R21 NS096402 and DOD-NFRP W81XWH-16-1-0220 (J.A.W.). NP is an investigator of HHMI. We thank the Sheffield RNAi Screening Facility, Biomedical Sciences, University of Sheffield, supported by the Wellcome Trust (grant reference number 084757) for providing RNAi libraries.

Competing Interest Statement: B.E.H. is a shareholder and founding director of Quest Genetics Ltd. The remaining authors declare no competing interests.

REFERENCES

1. Lawrence MS*, et al.* Discovery and saturation analysis of cancer genes across 21 tumour types. *Nature* **505**, 495-501 (2014).

2. Evans DG*, et al.* Birth incidence and prevalence of tumor-prone syndromes: estimates from a UK family genetic register service. *Am J Med Genet A* **152A**, 327-332 (2010).

3. Gutmann DH, Ferner RE, Listernick RH, Korf BR, Wolters PL, Johnson KJ. Neurofibromatosis type 1. *Nat Rev Dis Primers* **3**, 17004 (2017).

4. Rasmussen SA, Yang Q, Friedman JM. Mortality in neurofibromatosis 1: an analysis using U.S. death certificates. *Am J Hum Genet* **68**, 1110-1118 (2001).

5. Martin GA*, et al.* The GAP-related domain of the neurofibromatosis type 1 gene product interacts with ras p21. *Cell* **63**, 843-849 (1990).

6. Simanshu DK, Nissley DV, McCormick F. RAS Proteins and Their Regulators in Human Disease. *Cell* **170**, 17-33 (2017).

7. Gross AM*, et al.* Selumetinib in Children with Inoperable Plexiform Neurofibromas. *N Engl J Med* **382**, 1430-1442 (2020).

8. Baldo F, Magnolato A, Barbi E, Bruno I. Selumetinib side effects in children treated for plexiform neurofibromas: first case reports of peripheral edema and hair color change. *BMC Pediatr* **21**, 67 (2021).

9. Kaelin WG, Jr. The concept of synthetic lethality in the context of anticancer therapy. *Nat Rev Cancer* **5**, 689-698 (2005).

10. Lord CJ, Ashworth A. PARP inhibitors: Synthetic lethality in the clinic. *Science* **355**, 1152-1158 (2017).

11. Ryan CJ, Bajrami I, Lord CJ. Synthetic Lethality and Cancer - Penetrance as the Major Barrier. *Trends Cancer* **4**, 671-683 (2018).

749
750 12. Valvezan AJ*, et al.* mTORC1 Couples Nucleotide Synthesis to Nucleotide Demand Resulting in
751 a Targetable Metabolic Vulnerability. *Cancer Cell* **32**, 624-638 e625 (2017).

752
753 13. Nicholson HE*, et al.* HIF-independent synthetic lethality between CDK4/6 inhibition and VHL
754 loss across species. *Sci Signal* **12**, (2019).

755
756 14. Housden BE*, et al.* Identification of potential drug targets for tuberous sclerosis complex by
757 synthetic screens combining CRISPR-based knockouts with RNAi. *Sci Signal* **8**, rs9 (2015).

758
759 15. Housden BE*, et al.* Loss-of-function genetic tools for animal models: cross-species and cross-
760 platform differences. *Nat Rev Genet* **18**, 24-40 (2017).

761
762 16. Housden BE, Nicholson HE, Perrimon N. Synthetic Lethality Screens Using RNAi in Combination
763 with CRISPR-based Knockout in Drosophila Cells. *Bio Protoc* **7**, (2017).

764
765 17. Lee H*, et al.* DNA copy number evolution in Drosophila cell lines. *Genome Biol* **15**, R70 (2014).

766
767 18. Szklarczyk D*, et al.* STRING v11: protein-protein association networks with increased coverage,
768 supporting functional discovery in genome-wide experimental datasets. *Nucleic Acids Res* **47**,
769 D607-D613 (2019).

770
771 19. Housden BE*, et al.* Improved detection of synthetic lethal interactions in Drosophila cells using
772 variable dose analysis (VDA). *Proc Natl Acad Sci U S A* **114**, E10755-E10762 (2017).

773
774 20. Homewood CA, Warhurst DC, Peters W, Baggaley VC. Lysosomes, pH and the anti-malarial
775 action of chloroquine. *Nature* **235**, 50-52 (1972).

776
777 21. Mauvezin C, Neufeld TP. Bafilomycin A1 disrupts autophagic flux by inhibiting both V-ATPase-
778 dependent acidification and Ca-P60A/SERCA-dependent autophagosome-lysosome fusion.
779 *Autophagy* **11**, 1437-1438 (2015).

780
781 22. Levy JMM, Towers CG, Thorburn A. Targeting autophagy in cancer. *Nat Rev Cancer* **17**, 528-
782 542 (2017).

783
784 23. Kocaturk NM, Akkoc Y, Kig C, Bayraktar O, Gozuacik D, Kutlu O. Autophagy as a molecular
785 target for cancer treatment. *Eur J Pharm Sci* **134**, 116-137 (2019).

786
787 24. Li H, Chang LJ, Neubauer DR, Muir DF, Wallace MR. Immortalization of human normal and NF1
788 neurofibroma Schwann cells. *Lab Invest* **96**, 1105-1115 (2016).

789
790 25. King LB*, et al.* Developmental loss of neurofibromin across distributed neuronal circuits drives
791 excessive grooming in Drosophila. *PLoS Genet* **16**, e1008920 (2020).

792
793 26. Moscato EH, Dubowy C, Walker JA, Kayser MS. Social Behavioral Deficits with Loss of
794 Neurofibromin Emerge from Peripheral Chemosensory Neuron Dysfunction. *Cell Rep* **32**,
795 107856 (2020).

796
797 27. Bai L*, et al.* A Conserved Circadian Function for the Neurofibromatosis 1 Gene. *Cell Rep* **22**,
798 3416-3426 (2018).

799
800 28. Walker JA*, et al.* Genetic and functional studies implicate synaptic overgrowth and ring gland
801 cAMP/PKA signaling defects in the Drosophila melanogaster neurofibromatosis-1 growth
802 deficiency. *PLoS Genet* **9**, e1003958 (2013).

803
804 29. Gouzi JY*, et al.* The receptor tyrosine kinase Alk controls neurofibromin functions in Drosophila
805 growth and learning. *PLoS Genet* **7**, e1002281 (2011).

806
807 30. Markham A, Keam SJ. Selumetinib: First Approval. *Drugs* **80**, 931-937 (2020).

808
809 31. Zhang XJ, Chen S, Huang KX, Le WD. Why should autophagic flux be assessed? *Acta Pharmacol*
810 *Sin* **34**, 595-599 (2013).

811
812 32. Mizushima N, Levine B, Cuervo AM, Klionsky DJ. Autophagy fights disease through cellular self-
813 digestion. *Nature* **451**, 1069-1075 (2008).

814
815 33. O'Donovan TR, O'Sullivan GC, McKenna SL. Induction of autophagy by drug-resistant
816 esophageal cancer cells promotes their survival and recovery following treatment with
817 chemotherapeutics. *Autophagy* **7**, 509-524 (2011).

818
819 34. Peng X*, et al.* Autophagy promotes paclitaxel resistance of cervical cancer cells: involvement
820 of Warburg effect activated hypoxia-induced factor 1-alpha-mediated signaling. *Cell Death Dis*
821 **5**, e1367 (2014).

822
823 35. Zanotto-Filho A*, et al.* Autophagy inhibition improves the efficacy of curcumin/temozolomide
824 combination therapy in glioblastomas. *Cancer Lett* **358**, 220-231 (2015).

825
826 36. Golden EB*, et al.* Chloroquine enhances temozolomide cytotoxicity in malignant gliomas by
827 blocking autophagy. *Neurosurg Focus* **37**, E12 (2014).

828
829 37. Mei L*, et al.* Synergistic anti-tumour effects of tetrandrine and chloroquine combination
830 therapy in human cancer: a potential antagonistic role for p21. *Br J Pharmacol* **172**, 2232-2245
831 (2015).

832
833 38. Farrow JM, Yang JC, Evans CP. Autophagy as a modulator and target in prostate cancer. *Nat*
834 *Rev Urol* **11**, 508-516 (2014).

835

836 39. Lefort S*, et al.* Inhibition of autophagy as a new means of improving chemotherapy efficiency
837 in high-LC3B triple-negative breast cancers. *Autophagy* **10**, 2122-2142 (2014).

838
839 40. Yang A, Kimmelman AC. Inhibition of autophagy attenuates pancreatic cancer growth
840 independent of TP53/TRP53 status. *Autophagy* **10**, 1683-1684 (2014).

841
842 41. Jia L, Wang J, Wu T, Wu J, Ling J, Cheng B. In vitro and in vivo antitumor effects of chloroquine
843 on oral squamous cell carcinoma. *Mol Med Rep* **16**, 5779-5786 (2017).

844
845 42. Eng CH*, et al.* Macroautophagy is dispensable for growth of KRAS mutant tumors and
846 chloroquine efficacy. *Proc Natl Acad Sci U S A* **113**, 182-187 (2016).

847
848 43. Schmukler E, Kloog Y, Pinkas-Kramarski R. Ras and autophagy in cancer development and
849 therapy. *Oncotarget* **5**, 577-586 (2014).

850
851 44. Guo JY*, et al.* Activated Ras requires autophagy to maintain oxidative metabolism and
852 tumorigenesis. *Genes Dev* **25**, 460-470 (2011).

853
854 45. Morgan MJ*, et al.* Regulation of autophagy and chloroquine sensitivity by oncogenic RAS in
855 vitro is context-dependent. *Autophagy* **10**, 1814-1826 (2014).

856
857 46. Yuan N*, et al.* Bafilomycin A1 targets both autophagy and apoptosis pathways in pediatric B-
858 cell acute lymphoblastic leukemia. *Haematologica* **100**, 345-356 (2015).

859
860 47. Ohta T*, et al.* Bafilomycin A1 induces apoptosis in the human pancreatic cancer cell line Capan-
861 1. *J Pathol* **185**, 324-330 (1998).

862
863 48. Downward J. Targeting RAS signalling pathways in cancer therapy. *Nat Rev Cancer* **3**, 11-22
864 (2003).

865
866 49. Kinsey CG*, et al.* Protective autophagy elicited by RAF-->MEK-->ERK inhibition suggests a
867 treatment strategy for RAS-driven cancers. *Nat Med* **25**, 620-627 (2019).

868
869 50. Fishbein L*, et al.* In vitro studies of steroid hormones in neurofibromatosis 1 tumors and
870 Schwann cells. *Mol Carcinog* **46**, 512-523 (2007).

871
872 51. Sierzputowska K, Baxter CR, Housden BE. Variable Dose Analysis: A Novel High-throughput
873 RNAi Screening Method for Drosophila Cells. *Bio Protoc* **8**, e3112 (2018).

874
875 52. Ren X*, et al.* Optimized gene editing technology for Drosophila melanogaster using germ line-
876 specific Cas9. *Proc Natl Acad Sci U S A* **110**, 19012-19017 (2013).

877

878 53. Walker JA*, et al.* Reduced growth of Drosophila neurofibromatosis 1 mutants reflects a non-
879 cell-autonomous requirement for GTPase-Activating Protein activity in larval neurons. *Genes*
880 *Dev* **20**, 3311-3323 (2006).

881
882 54. Dietzl G*, et al.* A genome-wide transgenic RNAi library for conditional gene inactivation in
883 Drosophila. *Nature* **448**, 151-156 (2007).

884
885 55. The I*, et al.* Rescue of a Drosophila NF1 mutant phenotype by protein kinase A. *Science* **276**,
886 791-794 (1997).

887

888

889

890

891

SUPPLEMENTAL INFORMATION

Table S1. The genome-wide dsRNA screen identified 134 synthetic lethal partner genes to NF1

Table S2. Further screening of the 134 synthetic lethal partner genes identified 54 candidate genes with human orthologs

Fig. S1. The *NF1* gene is well conserved between *Drosophila* and humans with 68% identity at the amino acid level. Alignment of amino acid sequences of neurofibromin from human (isoform 2, NP_000258.1) and *Drosophila* (PB isoform, Flybase ID: FBpp0084326) using Clustal Omega. Colors represent: RED - small + hydrophobic: (AVFPMILW (including aromatic -Y)); BLUE - Acidic (DE); MAGENTA - Basic (RK -H); GREEN: hydroxyl + sulfhydryl + amine + G (STYHCNGQ). (*) indicates identical amino acids; (:) conserved substitutions; (.) semi-conserved substitutions. The boxed region indicates the GAP-related domain (GRD) encompassing residues 1170-1530 (human) and 1214-1575 (*Drosophila*).

```
Human   MAAHRPVEWVQAVVSRFDEQLPIKTGQQNTHTKVSTEHNKECLINISKYKFSLVISGLTT 60
Dros    -MTQKPGEWASALLARFEDQLPNRIGAYGTQARMSQDQLVACLIHISRYRFSLVISGLTK 59

Human   ILKNVNNMRIFGEAAEKN-LYLSQLIILDTLEKCLAGQPKDTMRLDETMLVKQLLPEICH 119
Dros    MLQRVNEAALQNRHEPERCYFESLVIILTTLERCLTNQTKDTARFEEAMNVKLLLREISQ 119

Human   FLHTCREGNQHAAELRNSASGVLFSLSCNNFNAVFSRISTRLQELTVCSEDNVDVHDIEL 179
Dros    FVDVQSDSNPNAAQLKALASKVLFALSQNHFSAVFNRISARIQELTSCSEENPDYNDIEL 179

Human   LQYINVDCAKLKRLLKETAFKFKALKKVAQLAVINSLEKAFWNWVENYPDEFTKLYQIPQ 239
Dros    IQHIDMDMIKLTKLLQETITKFRSK-RAPPLILLYSLEKAIWNWIEYHPQEFQDLQRGTN 238

Human   TDMAECAEKLFDLVDGFAES-TKRKAAVWPLQIILLILCPEIIQDISKDVV---------- 289
Dros    RDISTCWEPLMDFVEYFKTENKKSKTLVWPLQMLLLILNPSCLEAVVNELQQSEKEKEKD 298

Human   --------------DENNMNKKLFLDSLRKALAGHGGSRQLTESAAIACVKLCKASTYINW 336
Dros    KEKVASKSAQSTSRDKDFSAKQFIESIKRGLGQHSPSKQVTESAAIACVKLCKASTYINN 358

Human   ED-NSVIFLLVQSMVVDLKNLLFNPSKPFSRGSQ--PADVDLMIDCLVSCFRISPHNNQH 393
Dros    TDSNNVVFKLVQFFINDLKALLFNPAKPFSRGQGYNFADIELMIDCWVSCFRINPHNIEA 418

Human   FKICLAQNSPSTFHYYLVNSLH--------------------RIITNSALDWWPKIDAVYCHS 436
Dros    LKVCLNLSSPQAYHFVIVCSLLRLAHIYVDFRLQNKNPFRIVNQPRLSWWPQTDVVHYRS 478

Human   VELRNMFGETLHKAVQGCGAHPAIRMAPSLTFKEKVTSLKFKEKPTDLETRSYKYLLLSM 496
Dros    AELRALFTDTLNKATQGYIAHTPLRYITSLTLKSKDTQKGLTR----AEEGPAHKMLLLLL 535

Human   VKLIHADPKLLLCNPRKQGPETQGSTAELITGLVQLVPQSHMPEIAQEAMEALLVLHQLD 556
Dros    VRLIHADPTLLLNTQGKVAHEVQSSTLELINGLVSLVHQTTMPDVAQEAMEALLALHAPE 595

Human   SIDLWNPDAPVETFWEISSQMLFYICKKLTSHQMLSSTEILKWLREILICRNKFLLKNKQ 616
Dros    KIEVWNPEAPINTFWDVSSQVLFSISQKLIQHQIANYTDVLKWLREILICRNTFLQRHKD 655

Human   ADRSSCHFLLFYGVGCDIPSSGNTSQMSMDHEELLRTPGASLRKGKGNSSMDSAAGCSGT 676
Dros    YAH-------------------------------------------------------VGSQ 662

Human   PPICRQAQTKLEVALYMFLWNPDTEAVLVAMSCFRHLCEEADIRCGVDEVSVHNLLPNYN 736
Dros    IAICKQAHIKMEVVFFMYLWSVDLDAVLTSLSCFGLLCEEAEICCSSDELTVGFIMPNYH 722

Human   TFMEFASVSNMMS----------------TGRAALQKRVMALLRRIEHPTAGNTEAWEDTHA 782
Dros    IYQELAQLSTSATDSRICFFDNTHGNVLSRLTLQKRIMTLLRKIEHCVHGVQPAWEETFR 782

Human   KWEQATKLILNYPKAKMEDGQAAESLHKTIVKRRMSHVSGGGSIDLSDTDSLQEWINMTG 842
Dros    NWEVSSKVLQTYPKCKGEDGQA-EVFHRGMGKRRASHQSSEHD-----LEEQINEWANMTW 837

Human   FLCALGGVCLQQRSNSGLATYSPP------MGPVS------------ERKGSM----------I 878
Dros    FLLALGGVCLHKRSSSRQMLLQQSQNNASLGSLAQNSLYSSSTSSGHGSLHPSTVSLSTL 897

Human   SVMSSEGNADTPVSKFMDRLLSLMVCNHEKVGLQIRTNVKDLVGLELSPALYPMLFNKLK 938
Dros    PPAPPQDVSYCPVTQFVGQLLRLLVCSNEKIGLNIQKNVKELVGEEMSTQLYPILFDQVR 957

Human   NTISKFFDSQGQVL--LTDTNTQFVEQTIAIMKNLLDNH----------TEGSSEHLGQASI 988
Dros    AIVEKFFDQQGQVNVNVTDINTQFIEHTIYIMKSILDPKANKDPNNDQPSPSEHLGVTSI 1017

Human   ETMMLNLVRYVRVLGNMVHAIQIKTKLCQLVEVMMARRDDLSFCQEMKFRNKMVEYLTDW 1048
Dros    EGMMLGIVRYVRHLDMTVYAIRIKTKLCQLVEVMMKRRDDLAFRQEMKFRNKLVEYLTDW 1077

Human   VMGTSNQAADD----------DVKCLTRDLDQASMEAVVSLLAGLPLQPEEGDGVELMEAK 1099
Dros    VMGTSHQIAPPSSADAAILTNTSLIFRDLDQACMEAVAALLRGLPLQPEESDRGDLMDAK 1137

Human   SQLFLKYFTLFMNLLNDCSEVEDESAQT-------GGRKRGMSRRLASLRHCTVLAMSNLL 1153
Dros    SALFLKYFTLFMNLLNDCIDSSEAEKEMNNTPLLPPRPRMAAGKLTALRNATILAMSNLL 1197

Human   NANVDSGLMHSIGLGYHKDLQTRATFMEVLTKILQQGTEFDTLAETVLADRFERLVELVT 1213
Dros    GANIDSGLMHSIDLGYNPDLQTRAAFMEVLTQILQQGTEFDTLAETVLADRFEQLVQLVT 1257

Human   MMGDQGELPIAMALANVVPCSQWDELARVLVTLFDSRHLLYQLLWNMFSKEVELADSMQT 1273
Dros    MISDKGELPIAMALANVVTTSQMDELARVLVTLFDAKHLLSPLLWNMFYREVEVSDCMQT 1317

Human   LFRGNSLASKIMTFCFKVYGATYLQKLLDPLLRIVITSSDWQHVSFEVDPTRLEPSESLE 1333
Dros    LFRGNSLGSKIMAFCFKIYGASYLQMLLEPLIRPLLDEE---EETCFEVDPARLDPTEDIE 1375

Human   ENQRNLLQMTEKFFHAIISSSSEFPPQLRSVCHCLYQVVSQRFP----QNSIGAVGSAMFL 1390
Dros    QHRNNLIALTQKVFDAIINSSDRFPPQLRSMCHCLYQVLSKRFPNLLQNNIGAVGTVIFL 1435

Human   RFINPAIVSPYEAGILDKKPPPRIERGLKLMSKILQSIANHVLFTKEEHMRPFNDFVKSN 1450
Dros    RFINPAIVSPQELGIVDKQVHSSAKRGLMLMSKILQNIANHVEFSKEQHMLCFNDFLRDH 1495

Human   FDAARRFFLDIASDCPTSDAVNHSLSFISDGNVLALHRLLWNNQEKIGQYLSSNRDHKAV 1510
Dros    FEAGRRFFIQIASDCETVDQTSHSMSFISDANVLALHRLLWTHQEKIGDYLSSSRDHKAV 1555

Human   GRRPFDKMATLLAYLGPPEHKPVAD--------THWSSLNLTSSKFEEFMTRHQVHEKEEF 1563
Dros    GRRPFDKMATLLAYLGPPEHKPVDSHMMFSSYARWSSIDMSSTNFEEIMVKHQMHEKEEF 1615

Human   KALKTLSIFYQAGTSKAGNPIFYYYARRFKTGQINGDLLIYHVLLTLKPYYAKPYEIVVD 1623
Dros    KTLKSMNIFYQAGTSKSGYPVFYYIARRYKIGETNGDLLIYHVILTLKPFCHSPFEVVID 1675

Human   LTHTGPSNRFKTDFLSKWFVVFPGFAYDNVSAVYIYNCNSWVREYTKYHERLLTGLKGSK 1683
Dros    FTHTCSDNRFRTEFLQKWFYVLPTVAYENVHAVYIYNCNSWVREYTKFHDRILAPLKGNR 1735

Human   RLVFIDCPGKLAEHIEHEQQKLPAATLALEEDLKVFHNALKLAHKDTKVSIKVGSTAVQV 1743
Dros    KLLFLESPNKLTDFIDAEQQKLPGATLSLDEDLKVFSNALKLSHKDTKVAIKVGPTALQI 1795

Human   TSAERTKVLGQSVFLNDIYYASEIEEICLVDENQFTLTIANQGTPLTFMHQECEAIVQSI 1803
Dros    TSAEKTKVLAHSVLLNDVYYASEIEEVCLVDDNQFTLSITNESGQLSFIHNDCDNIVQAI 1855

Human   IHIRTRWELSQPDSIPQHTKIRPKDVPGTLLNIALLNLGSSDPSLRSAAYNLLCALTCTF 1863
Dros    IHIRNRWELSQPDSVTVHQKIRPKDVPGTLLNMALLNLGSCDPNLRTAAYNLLCALTATF 1915

Human   NLKIEGQLLETSGLCIPANNTLFIVSISKTLAANEPHLTLEFLEECISGFSKSSIELKHL 1923
Dros    DLKIEGQLLETQGLCIPSNNTIFIKSVSEKLATNEPHLTLEFLEESIQGFQRSTIELKHL 1975

Human   CLEYMTPWLSNLVRFCKHNDDAKRQRVTAILDKLITMTINEKQMYPSIQAKIWGSLGQIT 1983
Dros    CLEYMTPWLKNLVKFCKSNDDSKKLKVSQILDKLINLTIDQKEMYPSVQAKIWGSIGQIP 2035

Human   DLLDVVLDSFIKTSATGGLGSIKAEVMADTAVALASGNVKLVSSKVIGRMCKIIDKTCLS 2043
Dros    ELIDMVLDNFLHKSITYGLGSPQVEIMADTAVALASANVQLVSKKVITRICRVMDKSCTN 2095

Human   PTPTLEQHLMWDDIAILARYMLMLSFNNSLDVAAHLPYLFHVVTFLVATGPLSLRASTHG 2103
Dros    PTQYLEQHMMWDDIAILGRYLLMLSFNNCLDVATSVPYLFHTITFLVCSGGSLSMRASTHG 2155

Human   LVINIIHSLCTCSQLHFSEETKQVLRLSLTEFSLPKFYLLFGISKVKSAAVIAFRSSYRD 2163
Dros    LVINIIHSLCTCTNPSFSEEAQRVLRLSLDEFSLPKFYLLFGISKVKSAAVTAFRSSCRH 2215

Human   R----------SFSPGSYERETFALTSLETVTEALLEIMEACMRDIPTCKWLDQWTELAQR 2214
Dros    PTDKWLGNERVTQPLPADRERLSLPSLEVITDALLEIMEACMRDVPDCEWLNTWTSLARS 2275

Human   FAFQYNPSLQPRALVVFGCISKRVSHGQIKQIIRILSKALESCLKGPDTYNSQVLIEATV 2274
Dros    FAFCYNPALQPRALIVYGCISKSVTDHEVKQLLRILVKALE--------SFNDLILIEALV 2328

Human   IALTKLQPLLNKDSPLHKALFWVAVAVLQLDEVNLYSAGTALLEQNLHTLDSLRIFNDKS 2334
Dros    MCLTRIQPLLRPESPIHRALFWVAISVLQLDEITLYGAGLALLEQNLHTLKSQGCFDKKE 2388

Human   -PEEVFMAIRNPLEWHCKQMDHFVGLNFNSNFNFALVGHLLKGYRHPSPAIVARTVRILH 2393
Dros    TIAEVMMKTREKLEWHFKQLDHAVGLSFRSNFHFALVGHLIKGFRHPTPTTVSRTSRVLT 2448

Human   TLLTLVNKHRNCDKFEVNTQSVAYLAALLTVSEEVRSRCSLKHRKSLLLTDISMENVPMD 2453
Dros    MLLGIIAKPLHRDKFEVTPDSVAYLTALVAVSEEVRSRCHVKHALPRWPADLSSSV---- 2504

Human   TYPIHHGDPSYRT--------LKETQPWSSPKGSEGYLAATYPTVGQTSPRARKSMSLDMG 2506
Dros    -----ENGEASGGVQAIGLPLSRRQKSWDILDQSALQ--------------------FARQHK 2542

Human   QPSQANTKKLLGTRKSFDHLISDTKAPKRQEMESGITTPPKMRRVAETDYEMETQRISSS 2566
Dros    VPTLQNARVLFKTQRSFSVPT--TKDPN---NATGI-------------------------EE 2575

Human   QQHPHLRKVSVSESNVLLDEEVLTDPKIQALLLTVLATLVKYTTDEFDQRILYEYLAEAS 2626
Dros    RQERGSRSSVSNESNVLLDPEVLPDLSIQALVLTVLATLVKYSSDEGETRVLYQYLAEGS 2635

Human   VVFPKVFPVVHNLLDSKINTLLSLCQDPNLLNPIHGIVQSVVYHEESPPQYQTSYLQSFG 2686
Dros    VVFPKVFPVIHSLLDQKINNILSVSHDQVVLNSVONIIQNMLA-SEDPSQQQLHFLQSCG 2694

Human   FNGLWRFAGPFSKQTQIPDYAELIVKFLDALIDTYLPGIDEETSEESLLTPTSPYPPALQ 2746
Dros    FGGLWRFAGPFTKYNMMGESSELFVNCLEAMVETCLPGDESAP-------VPPSPRPYNLS 2748

Human   SQLSITA---NLN----------LSNSMTSLATSQHSPGIDKENVELSPTTGHCNSG 2790
Dros    SSLSSLTLGSPTDKAFSSESLDFYDNCPGSVSSLRRASHSKSRAKHRINDSPSH------ 2802

Human   RTRHGSASQVQKQRSAGSFKRNSIKKIV 2818
Dros    ------------------------------ 2802
```

908

Fig. S2. Drug dose curves. (A) Dose curves for the 15 drugs with *Drosophila* orthologs as targets in WT and NF1-KO S2R+ cells. **(B)** Dose curves for CQ and bafilomycin A1 in human CRISPR/Cas9 genome edited Schwann cells ($NF1^{+/-}$ and $NF1^{-/-}$). **(C)** Dose curves for CQ and bafilomycin A1 in human patient cells: ipnNF95.11C ($NF1^{+/-}$) and ipNF95.11b 'C' ($NF1^{-/-}$).

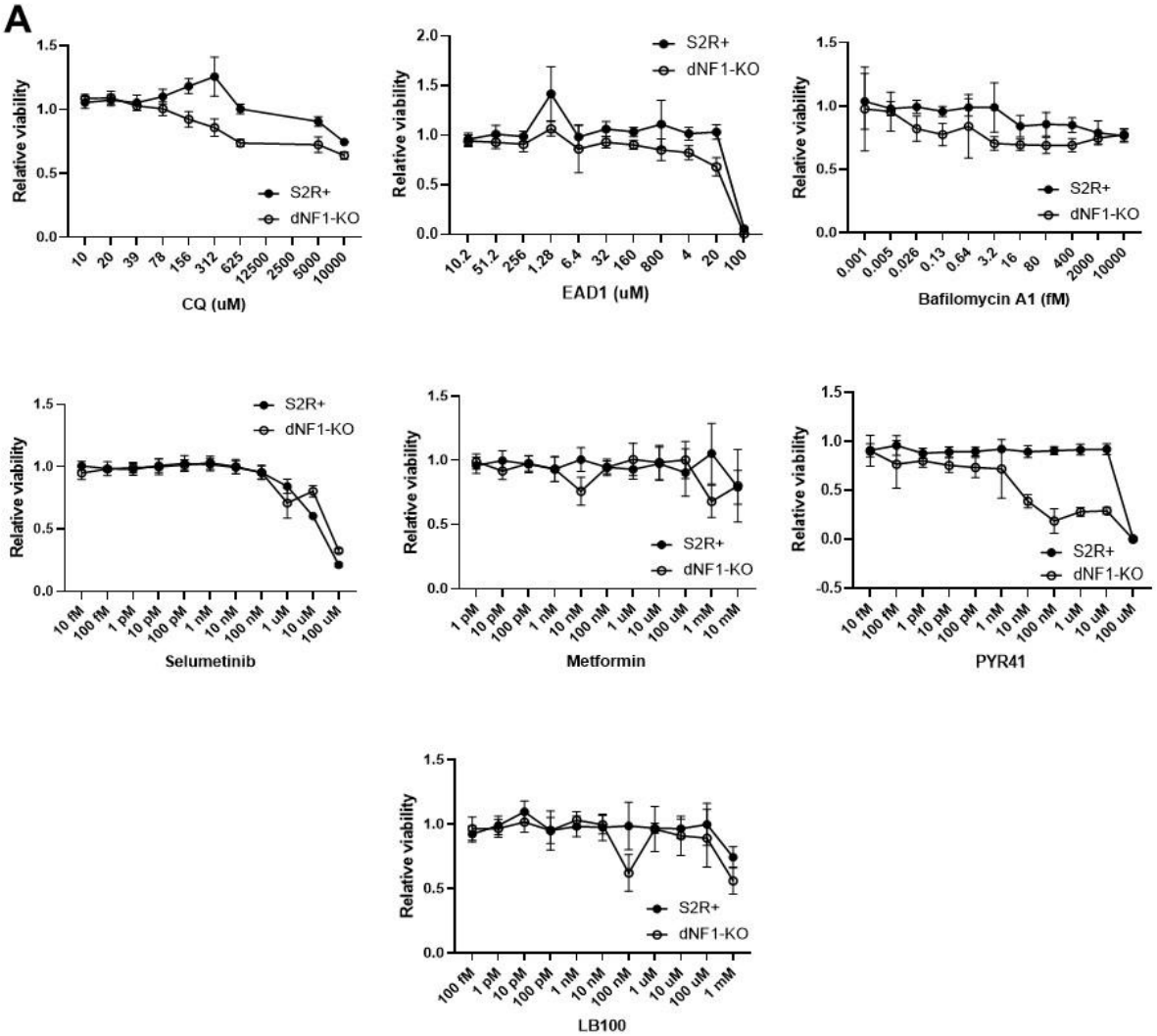

B

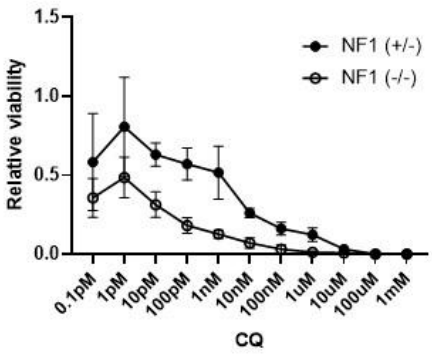
NF1 (+/-)
NF1 (-/-)
Relative viability
1.5
1.0
0.5
0.0
0.1pM
1pM
10pM
100pM
1nM
10nM
100nM
1uM
10uM
100uM
1mM
CQ

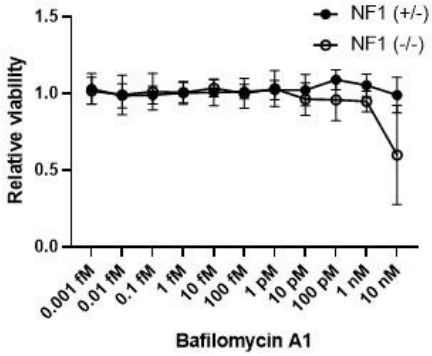
NF1 (+/-)
NF1 (-/-)
Relative viability
1.5
1.0
0.5
0.0
0.001 fM
0.01 fM
0.1 fM
1 fM
10 fM
100 fM
1 pM
10 pM
100 pM
1 nM
10 nM
Bafilomycin A1

C

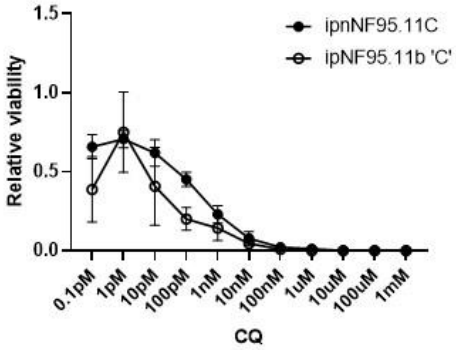
ipnNF95.11C
ipNF95.11b 'C'
Relative viability
1.5
1.0
0.5
0.0
0.1pM
1pM
10pM
100pM
1nM
10nM
100nM
1uM
10uM
100uM
1mM
CQ

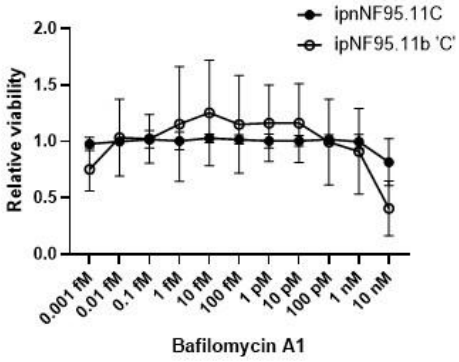
ipnNF95.11C
ipNF95.11b 'C'
Relative viability
2.0
1.5
1.0
0.5
0.0
0.001 fM
0.01 fM
0.1 fM
1 fM
10 fM
100 fM
1 pM
10 pM
100 pM
1 nM
10 nM
Bafilomycin A1

915